

# 1 Future snowfall in the Alps: Projections based on the EURO- 2 CORDEX regional climate models

3 Prisco Frei, Sven Kotlarski, Mark A. Liniger, Christoph Schär  
4  
5

## 6 - Second response to Referees – 7

### 8 General

9 We thank both referees for another thorough check of the revised manuscript. We're happy about the overall  
10 positive feedback, but also sorry about the fact the we could not address all concerns of referee #3 satisfactorily  
11 so far. As a consequence we have further revised the manuscript, please see the more detailed replies below.  
12 The most important change to the paper is a revised set of climate model simulations that are considered. All  
13 suggested further minor changes have been incorporated. We hope that the updated version of the paper raises  
14 no more concerns.

15 With kind regards, Sven Kotlarski (on behalf of all co-authors)

### 16 Response to Reviewer 2

17 **Comment** *Dear Authors, the revised manuscript has been improved a lot, all the major points have been adequately addressed*  
18 *in the reply to the Reviewers and eventually integrated in the main text. After the correction of the few typos listed below, I think*  
19 *this version of the manuscript is suitable for publication.*

20 *Congratulations for this nice paper!*

21 *Kind regards*

22 **Response and changes to manuscript** Thank you very much for the positive feedback. All suggested changes  
23 to the manuscript except have been incorporated.

24 **Comment** *Line 96: throughout the annual cycle -> throughout the year".*

25 **Response and changes to manuscript** Corrected.

26 **Comment** *Line 105: "on an RCM grid" -> on "the" RCM grid.*

27 **Response and changes to manuscript** Corrected.

28 **Comment** *Line 129: "the very focus" -> "the focus"*

29 **Response and changes to manuscript** Corrected.

30 **Comment** *Line 130: "on the snow projection aspect" -> "on snow projections"*

31 **Response and changes to manuscript** Corrected.

32 **Comment** *Line 138: "To estimate observation-based snowfall" sounds like an oxymoron, I suggest: "To estimate the reference*  
33 *fine-scale snowfall"*

34 **Response and changes to manuscript** Corrected.

35 **Comment** *Line 230: "not all RCM simulations available through EURO-CORDEX provide raw snowfall" -> "not all*  
36 *EUROCORDEX RCMs provide raw snowfall"*

37 **Response and changes to manuscript** Corrected.

38 **Comment** *Page 12: missing reference to Figure S5.*

39 **Response and changes to manuscript** Sorry, this was indeed a mistake. The figure should have been  
40 referenced in Section 3.2. We have now added the reference (note that the Figure is now called S6 instead of  
41 S5).

42 **Comment** Line 452: "partly explain the partly substantial overestimation"

43 **Response and changes to manuscript** Corrected.

44 **Comment** Line 713: "In" -> in

45 **Response and changes to manuscript** Corrected.

46 **Comment** Line 731: "the an"

47 **Response and changes to manuscript** Corrected.

48 **Comment** Line 735: "on an" -> "on the"

49 **Response and changes to manuscript** Corrected.

50 **Comment** Line: 783: "This effect ... may be strong under conditions (depending upon location and season) where the current  
51 climate is well below freezing. Such conditions may experience a shift towards a temperature range more favourable to  
52 snowfall". Maybe the word "conditions" is not the best choice here, can you please rephrase?

53 **Response and changes to manuscript** You are perfectly right. We rephrased the second sentence.

54 **Comment** Figure 2: the caption is unclear, you could rephrase "Ratio of a) mean snowfall Smean, b) heavy snowfall Sq99  
55 obtained with the Binary and the Richardson methods to the corresponding values obtained with the Subgrid method ..."

56 **Response and changes to manuscript** We did not change this specific sentence, but clarified the previous  
57 sentence (the meaning of the ratios is explained in there).

58

### 59 **Response to Reviewer 3**

60 **Comment** In my review of the original manuscript a couple of months ago I raised a couple of major points which in my opinion  
61 needed attention. Having read the revised manuscript and the accompanying rebuttal letter I notice that the authors have done  
62 a considerable effort to address all issues, also those from the other reviewers. Overall, the revisions have resulted in an  
63 improved manuscript. Unfortunately, not all comments have been adequately addressed, therefore some further attention is  
64 needed before the manuscript is suitable for publication.

65 **Response and changes to manuscript** Thanks very much for this feedback on our revisions. We're sorry that  
66 individual comments were not properly addressed in the reviewer's opinion. In the revised version we tried to  
67 further improve the manuscript in this respect and tried to incorporate all suggested changes. We hope and  
68 believe that the newly revised version is acceptable now.

69

70 **Comment** 1. (also point 1 in first review) The sentence added by the authors to point out that some works also utilized output  
71 from high resolution (12km) RCM output "It thereby complements ...(partly originating from EURO-CORDEX) ... but with a  
72 reduced ensemble size and/or not specifically targeting the entire Alpine region" I don't understand both phrases.

73 Firstly, EURO-CORDEX has a marginal role in both papers, and certainly nothing of the material and methodology originates  
74 from it. Just leave it out.

75 Secondly, these are both quite different studies, the Piazza et al. paper studies a variety of models in their response for a region  
76 in the French Alps., while the de Vries et al. paper utilizes a single-model 8-member ensemble considering a region including  
77 the entire Alpine region. I would advise to just explicitly phrase in what these papers primarily differ from your paper (i.e. region  
78 of analysis in Piazza et al. paper, and nature of model ensemble studied in de Vries et al.) and avoid using "and/or"  
79 constructions

80 **Response and changes to manuscript** We're sorry that our original corrections are not appropriate in the  
81 reviewer's opinion. We agree with the further points raised and modified the text according to the new  
82 suggestions.

83 **Comment** 2. (point 3 first review). I do not disagree that HadGEM2-RACMO has an issue with snow accumulation over the  
84 Alps, but this is rather the manifestation from a missing process (no glacier model) in combination with not setting an artificial  
85 limit on maximum snow depth (as is done in some of the other RCMs), than too much snow fall. Very large numbers in snow  
86 depth (or snow mass if available) are also seen in the model combinations EC-EARTH-HIRHAM, EC-EARTH-RACMO, and  
87 IPSL-WRF (in the first two even larger than in HadGEM2-RACMO), yet these combinations have been retained.

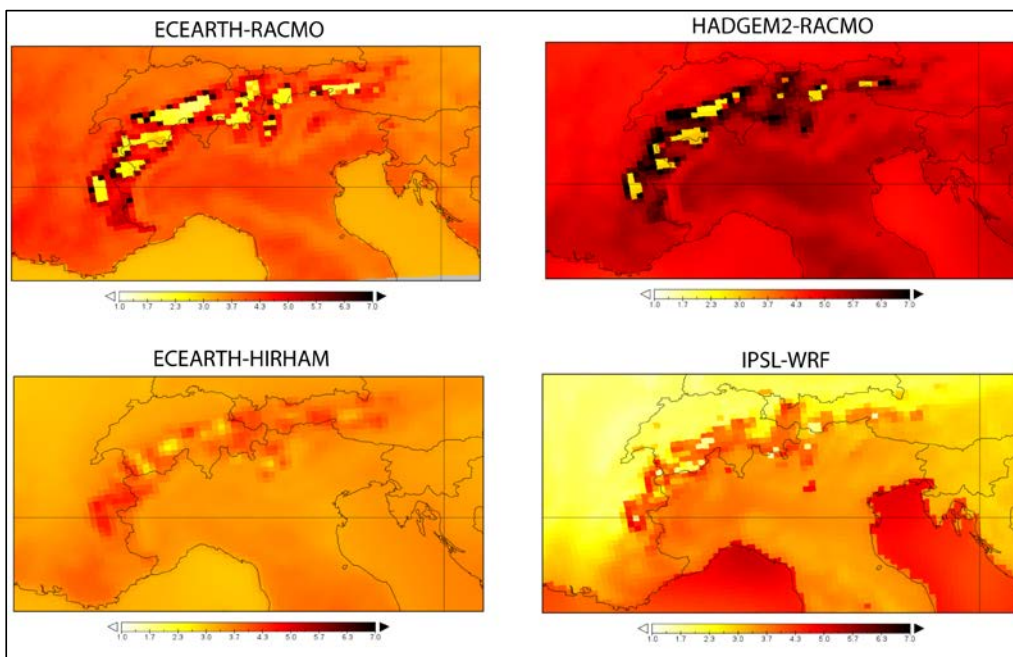
88 The authors furthermore mention in their rebuttal that the "obvious feedbacks on temperature" led them to disregard the  
89 HadGEM2-RACMO simulation. ". I would expect this to hold primarily for the summer season, and far less relevant in the winter  
90 season when sub-zero temperatures still dominate at the higher elevations where the anomalously high snow accumulation is  
91 found.

92 But even when it also affects the September-May season studied by the authors I don't see why the other three model  
93 combinations, mentioned above, don't suffer from this problem. After all, the sensitivity to temperature bias is to a large extent  
94 taken care of by the (bias-adjustment) shift in snow fractionation temperature  $T^*$  to  $T_a^*$ .

95 In my opinion the reason to disregard HadGEM2-RACMO is formulated rather ad hoc and could have been equally well been  
96 applied to disregard other model combinations which have now been retained. That leaves three options: 1) include HadGEM2-  
97 RACMO in the analysis, 2) disregard the other three combinations as well, or 3) provide a plausible explanation why this specific  
98 model combination was disregarded and other combinations not.

99 **Response and changes to manuscript** We are sorry that our original revisions to the paper were not considered  
100 as appropriate. We partly agree to the remaining comments of the reviewer. However, as we tried to describe in  
101 our previous replies, the snow accumulation in individual models itself is not problematic for our study as we're  
102 not employing simulated snow depth or simulated snow water equivalent. The problem here is the apparent  
103 feedback on the 2m temperature with adverse effects on the future temperature trend at individual grid cells. This  
104 problem cannot be overcome by our bias correction which is trained in the reference period and which does not  
105 account for non-stationary model biases. Hence, a widespread adverse influence on temperature trends in the  
106 analysis domain is an obvious reason to exclude the affected model chains from the analysis. The reviewer is  
107 right that this problem is most apparent in summer, but we cannot rule out effects in the transition seasons. The  
108 reviewer is also right in mentioning that further model chains are affected. This particularly concerns ECEARTH-  
109 RACMO (about 100 grid cells in the Alpine affected by snow accumulation), we are thankful for this comment. The  
110 problem is far less pronounced, however, for ECEARTH-HIRHAM (about 20 grid cells affected) and for IPSL-  
111 WRF (same order). Please see Figure R1 below for the spatial pattern of temperature changes by the end of the  
112 century for RCP8.5 and the four model chains under discussion. A widespread feedback of snow accumulation on  
113 2 temperature trends is obtained for both RACMO experiments. We therefore took these simulations out of our  
114 revised analysis. Following a further shortcoming of the IPSL-WRF experiment that was discovered in meantime  
115 (unphysical temperature change patterns) we also removed this model chain from our analysis, resulting in a total  
116 of 12 model chains analyzed (instead of 14). As a consequence, all results figures of the manuscript were  
117 adjusted, but the basic patterns do not change and the conclusions of the manuscript are not modified. The  
118 selection of experiments to be removed is now fully consistent with the upcoming CH2018 Swiss climate  
119 scenarios, it is documented on the CH2018 website [www.ch2018.ch](http://www.ch2018.ch) and in a specific model set documentation  
120 available from [http://www.ch2018.ch/wp-content/uploads/2017/07/CH2018\\_model\\_ensemble.pdf](http://www.ch2018.ch/wp-content/uploads/2017/07/CH2018_model_ensemble.pdf). The latter also  
121 provides more details on the reasons for removing individual experiments. The text Section 2.2 of the manuscript  
122 has been revised accordingly, as well as Table 1. A reference to the CH2018 website is provided.

123



124

125 **Fig. R 1** Temperature change signal over the Alpine region (2070-2099 wrt. 1981-2010) for four specific EUR-11 model chains (naming:  
126 GCM-RCM) and for RCP8.5.

127 **Comment 3.** (point 7 first review). The way the authors have addressed this point only makes things worse. I repeat that the line  
128 "Previous studies ... with this theory (e.g. Allen and Ingram, 2002; Ban et al. 2015)" is out of context, for reasons the authors  
129 agree on but refuse to act upon. What the authors do is adding a phrase which underlines that the material in their paper (daily

130 scales, no convection, cold season) is incompatible with the conditions studied in the Ban et al paper (sub-daily or hourly scales,  
131 convection, warm season), yet they state that their finding is consistent with the Ban et al..

132 An additional reason why I am emphasizing this point is that the literature on the projected behavior of hourly precipitation  
133 extremes under climate change is quite controversial, and far from settled at the moment (see also literature cited in Ban et al.  
134 2015). That aspect is entirely ignored in the current formulation, which is unacceptable.

135 I therefore stick to my point made in the first review that this sentence including the corresponding references must be taken out.

136 **Response and changes to manuscript** We apologize, it appears this is a misunderstanding. It is correct that the  
137 main emphasis of Ban et al. (2015) is on hourly precipitation scaling (and this is not addressed in the current  
138 study). However, the paper also considered the scaling of daily precipitation events. It has not been the intent of  
139 our revisions to focus on hourly time scales. We have clarified the statements correspondingly. To avoid  
140 confusion, we now reference a recently accepted publication (Rajczak et al. 2017) that entirely addresses daily  
141 time scales, instead of Ban et al. (2015).

142 **Comment** (point 28 in the first review) I meant to add an ancillary line showing the frequency of occurrence of the elevation  
143 intervals across the region of interest (either Switzerland or the Alpine region or both). Evidently the higher elevations are (far)  
144 less abundant than the lower elevations – there will be only very few grid cells with elevation beyond 3000 m a.s.l. , making the  
145 analysis for high elevation less robust. It would help to give an impression of the pdf of the elevations, you could use the upper  
146 horizontal axis to label the percentage. The attached png-file shows what I meant to say (only intervals above 250m are  
147 counted), the authors could plug in such line in Fig 3a, or, if they prefer in Fig 2, or Fig 4a, that is for them to choose.

148 **Response and changes to manuscript** Thanks very much for these further explanations, and sorry that the  
149 comment of the original review was not clear to us. We agree that this information would be helpful. However, we  
150 would prefer to introduce a separate figure on the area-elevation distribution rather than overloading existing  
151 figures with an additional line and an additional axis. We therefore added an additional figure (S2) to the  
152 supplementary material that shows the area-elevation distribution of the entire Alpine analysis domain based on  
153 the aggregated GTOPO30 elevation model. The figure is now referenced in Section 3.1 of the manuscript.

154 **Comment** (major point 4 first review) Indicate in Table 1 which EC-EARTH realizations are used (like you do for MPI-ESM-  
155 REMO) in the various EC-EARTH-RCM combinations: r11p1 for EC-EARTH-RACMO; r3i1p1 for EC-EARTH-HIRHAM; r12i1p1  
156 for EC-EARTH-SMHI and EC-EARTH-CCLM.

157 **Response and changes to manuscript** Done, thanks a lot. In addition, we provide the information on the  
158 realization of the driving GCM now in the column "GCM" instead of the column "Acronym". This is more  
159 appropriate in our opinion.

160 **Comment** Line 267: "leads a"  "leads to a"

161 **Response and changes to manuscript** Corrected.

162 **Comment** Line 300: rephrase "and as we condere ah as a" as "while ah is regarded as a ..."

163 **Response and changes to manuscript** Corrected.

164 **Comment** Line 328: rephrase "under current and future ... climate conditions" as "under changing ... climate conditions"

165 **Response and changes to manuscript** Corrected.

166

167 **New manuscript version with marked-up changes:**

168

## 169 **Future snowfall in the Alps: Projections based on** 170 **the EURO-CORDEX regional climate models**

171 Prisco Frei<sup>1</sup>, Sven Kotlarski<sup>2,\*</sup>, Mark A. Liniger<sup>2</sup>, Christoph Schär<sup>1</sup>  
172

173 <sup>1</sup>Institute for Atmospheric and Climate Sciences, ETH Zurich, CH-8006 Zurich, Switzerland

174 <sup>2</sup> Federal Office of Meteorology and Climatology, MeteoSwiss, CH-8058 Zurich-Airport,  
175 Switzerland

176

177 \* Corresponding author: [sven.kotlarski@meteoswiss.ch](mailto:sven.kotlarski@meteoswiss.ch)

178

179 **Abstract.** -Twenty-first century snowfall changes over the European Alps are assessed based  
180 on high-resolution regional climate model (RCM) data made available through the EURO-  
181 CORDEX initiative. Fourteen different combinations of global and regional climate models with  
182 a target resolution of 12 km, and two different emission scenarios are considered. As raw  
183 snowfall amounts are not provided by all RCMs, a newly developed method to separate  
184 snowfall from total precipitation based on near-surface temperature conditions and accounting  
185 for subgrid-scale topographic variability is employed. The evaluation of the simulated snowfall  
186 amounts against an observation-based reference indicates the ability of RCMs to capture the  
187 main characteristics of the snowfall seasonal cycle and its elevation dependency, but also  
188 reveals considerable positive biases especially at high elevations. These biases can partly be  
189 removed by the application of a dedicated RCM bias adjustment that separately considers  
190 temperature and precipitation biases.

191 Snowfall projections reveal a robust signal of decreasing snowfall amounts over most parts of  
192 the Alps for both emission scenarios. Domain and multi-model mean decreases of mean  
193 September-May snowfall by the end of the century amount to -25% and -45% for RCP4.5 and  
194 RCP8.5, respectively. Snowfall in low-lying areas in the Alpine forelands could be reduced by  
195 more than -80%. These decreases are driven by the projected warming and are strongly  
196 connected to an important decrease of snowfall frequency and snowfall fraction and are also  
197 apparent for heavy snowfall events. In contrast, high-elevation regions could experience slight  
198 snowfall increases in mid-winter for both emission scenarios despite the general decrease of  
199 the snowfall fraction. These increases in mean and heavy snowfall can be explained by a  
200 general increase of winter precipitation and by the fact that, with increasing temperatures,  
201 climatologically cold areas are shifted into a temperature interval which favours higher snowfall  
202 intensities. In general, percentage changes of snowfall indices are robust with respect to the  
203 RCM postprocessing strategy employed: Similar results are obtained for raw, separated and  
204 separated + bias-adjusted snowfall amounts. Absolute changes, however, can differ among  
205 these three methods.

206 **1 Introduction**

207 Snow is an important resource for the Alpine regions, be it for tourism, hydropower generation, or  
208 water management (Abegg et al., 2007). According to the Swiss Federal Office of Energy (SFOE)  
209 hydropower generation accounts for approximately 55% of the Swiss electricity production (SFOE,  
210 2014). Consideration of changes in snow climatology needs to address aspects of both snow cover  
211 and snowfall. In the recent past, an important decrease of the mean snow cover depth and duration in  
212 the Alps was observed (e.g. Laternser and Schneebeli, 2003; Marty, 2008; Scherrer et al., 2004).  
213 Projections of future snow cover changes based on climate model simulations indicate a further  
214 substantial reduction (Schmucki et al., 2015a; Steger et al., 2013), strongly linked to the expected rise  
215 of temperatures (e.g., CH2011, 2011; Gobiet et al., 2014). On regional and local scales rising  
216 temperatures exert a direct influence on snow cover in two ways: First, total snowfall sums are  
217 expected to decrease by a lower probability for precipitation to fall as snow implying a decreasing  
218 snowfall fraction (ratio between solid and total precipitation). Second, snow on the ground is subject to  
219 faster and accelerated melt. These warming-induced trends might be modulated by changes in  
220 atmospheric circulation patterns.

221 Although the snowfall fraction is expected to decrease during the 21st century (e.g., Räisänen, 2016)  
222 extraordinary snowfall events can still leave a trail of destruction. A recent example was the winter  
223 2013/2014 with record-breaking heavy snowfall events along the southern rim of the European Alps  
224 (e.g., Techel et al., 2015). The catastrophic effects of heavy snowfall range from avalanches and  
225 floods to road or rail damage. In extreme cases these events can even result in the weight-driven  
226 collapse of buildings or loss of human life (Marty and Blanchet, 2011). Also mean snowfall conditions,  
227 such as the mean number of snowfall days in a given period, can be of high relevance for road  
228 management (e.g. Zubler et al., 2015) or airport operation. Projections of future changes in snowfall,  
229 including mean and extreme conditions, are therefore highly relevant for long-term planning and  
230 adaptation purposes in order to assess and prevent related socio-economic impacts and costs.

231 21st century climate projections typically rely on climate models. For large-scale projections, global  
232 climate models (GCMs) with a rather coarse spatial resolution of 100 km or more are used. To assess  
233 regional to local scale impacts, where typically a much higher spatial resolution is required, a GCM  
234 can be dynamically downscaled by nesting a regional climate model (RCM) over the specific domain  
235 of interest (Giorgi, 1990). In such a setup, the GCM provides the lateral and sea surface boundary  
236 conditions to the RCM. One advantage of climate models is the ability to estimate climate change in a  
237 physically based manner under different greenhouse gas (GHG) emission scenarios. With the  
238 Intergovernmental Panel on Climate Change's (IPCC) release of the Fifth Assessment Report (AR5;  
239 IPCC, 2013) the so-called representative concentration pathway (RCP) scenarios have been  
240 introduced (Moss et al., 2010) which specify GHG concentrations and corresponding emission  
241 pathways for several radiative forcing targets. To estimate inherent projection uncertainties, ensemble  
242 approaches employing different climate models, different greenhouse gas scenarios, and/or different  
243 initial conditions are being used (e.g., Deser et al., 2012; Hawkins and Sutton, 2009; Rummukainen,  
244 2010).

245 Within the last few years several studies targeting the future global and European snowfall evolution  
246 based on climate model ensembles were carried out (e.g., de Vries et al., 2013; de Vries et al., 2014;  
247 Krasting et al., 2013; O’Gorman, 2014; Piazza et al., 2014; Räisänen, 2016; Soncini and Bocchiola,  
248 2011). Most of these analyses are based on GCM output or older generations of RCM ensembles at  
249 comparatively low spatial resolution, which are not able to properly resolve snowfall events over  
250 regions with complex topography. New generations of high resolution RCMs are a first step toward an  
251 improvement on this issue. This is in particular true for the most recent high-resolution regional climate  
252 change scenarios produced by the global CORDEX initiative (Giorgi et al., 2009) and its European  
253 branch EURO-CORDEX (Jacob et al., 2014). The present work aims to exploit this recently  
254 established multi-model RCM-archive with respect to future snowfall conditions over the area of the  
255 European Alps. It thereby complements the existing works of Piazza et al. (2014) and de Vries et al.  
256 (2014). These two works who among others also exploit comparatively high-resolved RCM  
257 experiments (partly originating from EURO-CORDEX as well) but with a smaller focus domain in the  
258 case of Piazza et al. (2014; French Alps only) and based on a single-model ensemble with a reduced  
259 comparatively small ensemble size (eight members) and/or not specifically targeting the entire Alpine  
260 region in the case of de Vries et al. (2014).

261 In general and on decadal to centennial time scales, two main drivers of future snowfall changes over  
262 the European Alps with competing effects on snowfall amounts are apparent from the available  
263 literature: (1) Mean winter precipitation is expected to increase over most parts of the European Alps  
264 and in most EURO-CORDEX experiments (e.g., Rajczak et al., 2017in-prep; Smiatek et al., 2016)  
265 which in principle could lead to higher snowfall amounts. (2) Temperatures are projected to  
266 considerably rise throughout the annual-cycle year (e.g., Gobiet et al., 2014; Smiatek et al., 2016;  
267 Steger et al., 2013) with the general effect of a decreasing snowfall frequency and fraction, thus  
268 potentially leading to a reduction in overall snowfall amounts. Separating the above two competing  
269 factors is one of the targets of the current study. A potential complication is that changes in daily  
270 precipitation frequency (here-events with precipitation > 1 mm/day) and precipitation intensity (average  
271 amount on wet days) can change in a counteracting manner (e.g., Fischer et al., 2015; Rajczak et al.,  
272 2013), and that relative changes are not uniform across the event category (e.g. Ban et al., 2015;  
273 Fischer and Knutti, 2016; Rajczak et al., 2017).

274 We here try to shed more light on these issues by addressing the following main objectives:

275 **Snowfall separation on thean RCM grid.** Raw snowfall outputs are not available for all members of  
276 the EURO-CORDEX RCM ensemble. Therefore, an adequate snowfall separation technique, i.e., the  
277 derivation of snowfall amounts based on readily available daily near-surface air temperature and  
278 precipitation data, is required. Furthermore, we seek for a snowfall separation method that accounts  
279 for the topographic subgrid-scale variability of snowfall on the RCM grid.

280 **Snowfall bias adjustment.** Even the latest generation of RCMs is known to suffer from systematic  
281 model biases (e.g., Kotlarski et al., 2014). In GCM-driven setups as employed within the present work  
282 these might partly be inherited from the driving GCM. To remove such systematic model biases in  
283 temperature and precipitation, a simple bias adjustment method is developed and employed in the

284 present work. To assess its performance and applicability, different snowfall indices in the bias-  
285 adjusted and not bias-adjusted output are compared against observation-based estimates.

286 **Snowfall projections for the late 21st century.** Climate change signals for various snowfall indices  
287 over the Alpine domain and for specific elevation intervals, derived by a comparison of 30-year control  
288 and scenario periods, are analysed under the assumption of the RCP8.5 emission scenario. In  
289 addition, we aim to identify and quantify the main drivers of future snowfall changes and, in order to  
290 assess emission scenario uncertainties, compare RCP8.5-based results with experiments assuming  
291 the more moderate RCP4.5 emission scenario. Snowfall projections are generally based on three  
292 different datasets: (1) raw RCM snowfall where available, (2) RCM snowfall separated from simulated  
293 temperature and precipitation, and (3) RCM snowfall separated from simulated temperature and  
294 precipitation and additionally bias-adjusted. While all three estimates are compared for the basic  
295 snowfall indices in order to assess the robustness of the projections, more detailed analyses are  
296 based on dataset (3) only.

297 In addition and as preparatory analysis, we carry out a basic evaluation of RCM-simulated snowfall  
298 amounts. This evaluation, however, is subject to considerable uncertainties as a high-quality  
299 observation-based reference at the required spatial scale is not available, and the ~~very~~-focus of the  
300 present work is laid on ~~the~~-snowfall projections~~s~~-aspect.

301 The article is structured as follows: Section 2 describes the data used and methods employed. In  
302 Sections 3 and 4 results of the bias adjustment approach and snowfall projections for the late 21st  
303 century are shown, respectively. The latter are further discussed in Section 5 while overall conclusions  
304 and a brief outlook are provided in Section 6. Additional supporting figures are provided in the  
305 supplementary material (prefix 'S' in Figure numbers).

## 306 **2 Data and methods**

### 307 **2.1 Observational data**

308 To estimate ~~observation-based-the reference fine-scale~~ snowfall, two gridded data sets, one for  
309 precipitation and one for temperature, derived from station observations and covering the area of  
310 Switzerland are used. Both data sets are available on a daily basis with a horizontal resolution of 2 km  
311 for the entire evaluation period 1971-2005 (see Sec. 2.3).

312 The gridded precipitation data set (RhiresD) represents a daily analysis based on a high-resolution  
313 rain-gauge network (MeteoSwiss, 2013a) consisting of more than 400 stations that have a balanced  
314 distribution in the horizontal but under-represent high altitudes (Frei and Schär, 1998; Isotta et al.,  
315 2014; Konzelmann et al., 2007). Albeit the data set's resolution of 2 km, the effective grid resolution as  
316 represented by the mean inter-station distance is about 15 - 20 km and thus comparable to the  
317 nominal resolution of the available climate model data (see Sec. 2.2). The dataset has not been  
318 corrected for the systematic measurement bias of rain gauges (e.g., Neff, 1977; Sevruk, 1985; Yang et  
319 al., 1999).



320 The gridded near-surface air temperature (from now on simply referred to as *temperature*) data set  
321 (TabsD) utilises a set of approx. 90 homogeneous long-term station series (MeteoSwiss, 2013b).  
322 Despite the high quality of the underlying station series, errors might be introduced by unresolved  
323 scales, an uneven spatial distribution and interpolation uncertainty (Frei, 2014). The unresolved effects  
324 of land cover or local topography, for instance, probably lead to an underestimation of spatial  
325 variability. Also note that, while RhiresD provides daily precipitation sums aggregated from 6 UTC to 6  
326 UTC of the following day, TabsD is a true daily temperature average from midnight UTC to midnight  
327 UTC. Due to a high temporal autocorrelation of daily mean temperature this slight inconsistency in the  
328 reference interval of the daily temperature and precipitation grids is expected to not systematically  
329 influence our analysis.

330 In addition to the gridded temperature and precipitation datasets and in order to validate simulated raw  
331 snowfall amounts station-based observations of fresh snow sums (snow depth) at daily resolution from  
332 29 stations in Switzerland with data available for at least 80% of the evaluation period 1971-2005 are  
333 employed.

## 334 2.2 Climate model data

335 In terms of climate model data we exploit a recent ensemble of regional climate projections made  
336 available by EURO-CORDEX ([www.euro-cordex.net](http://www.euro-cordex.net)), the European branch of the World Climate  
337 Research Programme's CORDEX initiative ([www.cordex.org](http://www.cordex.org); Giorgi et al., 2009). RCM simulations for  
338 the European domain were run at a resolution of approximately 50 km (EUR-44) and 12 km (EUR-11)  
339 with both re-analysis boundary forcing (Kotlarski et al., 2014; Vautard et al., 2013) and GCM-forcing  
340 (Jacob et al., 2014). We here disregard the reanalysis-driven experiments and employ the GCM-driven  
341 simulations only. These include historical control simulations and future projections based on RCP  
342 greenhouse gas and aerosol emission scenarios. Within the present work we employ daily averaged  
343 model output of GCM-driven EUR-11 simulations that were available in December 2016 and for which  
344 control, RCP4.5 and RCP8.5 runs are available. Individual available experiments were disregarded  
345 due to serious simulation shortcomings that potentially affect our analysis all-except two<sup>1</sup>GCM-driven  
346 EUR-11 simulations for which control, RCP4.5 and RCP8.5 runs were available in December 2016.  
347 This yields a total. The exclusion of these experiments is in line with the current set of experiments  
348 considered for the upcoming CH2018 Swiss climate scenarios ([www.ch2018.ch](http://www.ch2018.ch)). In total, a set of 124  
349 GCM-RCM model chains is considered, combining five driving GCMs with seven-five different RCMs  
350 (Tab. 1). We exclusively focus on the higher resolved EUR-11 simulations and disregard the coarser  
351 EUR-44 ensemble due to the apparent added value of the EUR-11 ensemble with respect to regional-  
352 scale climate features in the complex topographic setting of the European Alps (e.g., Giorgi et al.,  
353 2016; Torma et al., 2015).

---

<sup>1</sup> All experiments of the The HadGEM2-RACMO RCM experiments were excluded due to serious snow accumulation issues and evident feedbacks on 2m temperatures over the European Alps. Also, the IPSL-driven WRF simulations were disregarded due to suspicious and probably unphysical climate change signals in summer over the Alpine domain. Furthermore, only realization 1 of MPI-M-REMO was included in order to avoid mixing GCM-RCM sampling with pure internal climate variability sampling.

354 | It is important to note that each of the ~~seven-five~~ RCMs considered uses an individual grid cell  
355 | topography field. Model topographies for a given grid cell might therefore considerably differ from each  
356 | other, and also from the observation-based orography. Hence, it is not meaningful to compare snowfall  
357 | values at individual grid cells since the latter might be situated at different elevations. Therefore, most  
358 | analyses of the present work were carried out as a function of elevation, i.e., by averaging climatic  
359 | features over distinct elevation intervals.

### 360 **2.3 Analysis domain and periods**

361 | The arc-shaped European Alps - with a West-East extent of roughly 1200 km , a total of area 190'000  
362 | km<sup>2</sup> and -a peak elevation of 4810 m a.s.l. (Mont Blanc) - are the highest and most prominent  
363 | mountain range which is entirely situated in Europe. In the present work, two different analysis  
364 | domains are used. The evaluation of the bias adjustment approach depends on the observational data  
365 | sets RhiresD and TabsD (see Sec. 2.1). As these cover Switzerland only, the evaluation part of the  
366 | study (Sec. 3) is constrained to the Swiss domain (Fig. 1, bold line). For the analysis of projected  
367 | changes of different snowfall indices (Sec. 4 and 5) a larger domain covering the entire Alpine crest  
368 | with its forelands is considered (Fig. 1, coloured region).

369 | Our analysis is based on three different time intervals. The evaluation period (EVAL) 1971-2005 is  
370 | used for the calibration and validation of the bias adjustment approach. Future changes of snowfall  
371 | indices are computed by comparing a present-day control period (1981-2010, CTRL) to a future  
372 | scenario period at the end of the 21<sup>st</sup> century (2070-2099, SCEN). For all periods (EVAL, CTRL and  
373 | SCEN), the summer months June, July and August (JJA) are excluded from any statistical analysis. In  
374 | addition to seasonal mean snowfall conditions, i.e., averages over the nine-month period from  
375 | September to May, we also analyse the seasonal cycle of individual snowfall indices at monthly  
376 | resolution.

### 377 **2.4 Analysed snowfall indices and change signals**

378 | A set of six different snowfall indices is considered (Tab. 2). -Mean snowfall ( $S_{\text{mean}}$ ) refers to the  
379 | (spatio-) temporally-averaged snowfall amount in mm SWE (note that from this point on we will use the  
380 | term "mm" as a synonym for "mm SWE" as unit of several snowfall indices). The two indices heavy  
381 | snowfall ( $S_{q99}$ ) and maximum 1-day snowfall ( $S_{1d}$ ) allow the assessment of projected changes in heavy  
382 | snowfall events and amounts.  $S_{1d}$  is derived by averaging maximum 1-day snowfall amounts over all  
383 | individual months/seasons of a given time period (i.e., by averaging 30 maximum values in the case of  
384 | the CTRL and SCEN period), while  $S_{q99}$  is calculated from the grid point-based 99<sup>th</sup> all-day snowfall  
385 | percentile of the daily probability density function (PDF) for the entire time period considered. We use  
386 | all-day percentiles as the use of wet-day percentiles leads to conditional statements that are often  
387 | misleading (see the analysis in Schär et al. 2016). Note that the underlying number of days differs for  
388 | seasonal (September-May) and monthly analyses. Snowfall frequency ( $S_{\text{freq}}$ ) and mean snowfall  
389 | intensity ( $S_{\text{int}}$ ) are based on a wet-day threshold of 1 mm/day and provide additional information about  
390 | the distribution and magnitude of snowfall events, while the snowfall fraction ( $S_{\text{frac}}$ ) describes the ratio  
391 | of solid precipitation to total precipitation. As climate models tend to suffer from too high occurrence of

392 drizzle and as small precipitation amounts are difficult to measure, daily precipitation values smaller or  
393 equal to 0.1 mm were set to zero in both the observations and the simulations prior to the remaining  
394 analyses.

395 Projections are assessed by calculating two different types of changes between the CTRL and the  
396 SCEN period. The absolute change signal ( $\Delta$ ) of a particular snowfall index X (see Tab.2)

$$397 \quad \Delta X = X_{SCEN} - X_{CTRL} \quad (1)$$

398 and the relative change signal ( $\delta$ ) which describes the change of the snowfall index as a percentage of  
399 its CTRL period value

$$400 \quad \delta X = \left( \frac{X_{SCEN}}{X_{CTRL}} - 1 \right) \cdot 100 \quad (2)$$

401 To prevent erroneous data interpretation due to possibly large relative changes of small CTRL values,  
402 certain grid boxes were masked out before calculating and averaging the signal of change. This  
403 filtering was done by setting threshold values for individual indices and statistics (see-Table 2-).

## 404 2.5 Separating snowfall from total precipitation

405 Due to (a) the lack of a gridded observational snowfall data set and (b) the fact that not all EURO-  
406 CORDEX RCMs ~~simulations available through EURO-CORDEX~~ provide raw snowfall as an output  
407 variable, a method to separate solid from total precipitation depending on near-surface temperature  
408 conditions is developed. The simplest approach to separate snowfall from total precipitation is to  
409 fractionate the two phases binary by applying a constant snow fractionation temperature (e.g., de  
410 Vries et al., 2014; Schmucki et al., 2015a; Zubler et al., 2014). More sophisticated methods estimate  
411 the snow fraction  $f_s$  dependence on air temperature with linear or logistic relations (e.g., Kienzle, 2008;  
412 McAfee et al., 2014). In our case, the different horizontal resolutions of the observational (high  
413 resolution of 2 km) and simulated (coarser resolution of 12 km) data sets further complicate a proper  
414 comparison of the respective snowfall amounts. Thus, we explicitly analysed the snowfall amount  
415 dependency on the grid resolution and exploited possibilities for including subgrid-scale variability in  
416 snowfall separation. This approach is important as especially in Alpine terrain a strong subgrid-scale  
417 variability of near-surface temperatures due to orographic variability has to be expected, with  
418 corresponding effects on the subgrid-scale snowfall fraction.

419 For this preparatory analysis, which is entirely based on observational data, a reference snowfall is  
420 derived. It is based on the approximation of snowfall by application of a fixed temperature threshold to  
421 daily total precipitation amounts on the high resolution observational grid (2 km) and will be termed  
422 *Subgrid method* thereafter: First, the daily snowfall  $S'$  at each grid point of the observational data set at  
423 high resolution (2 km) is derived by applying a snow fractionation temperature  $T^*=2^\circ\text{C}$ . The whole  
424 daily precipitation amount  $P'$  is accounted for as snow  $S'$  (i.e.,  $f_s=100\%$ ) for days with daily mean  
425 temperature  $T \leq T^*$ . For days with  $T > T^*$ ,  $S'$  is set to zero and  $P'$  is attributed as rain (i.e.,  $f_s=0\%$ ). This  
426 threshold approach with a fractionation temperature of  $2^\circ\text{C}$  corresponds to the one applied in previous  
427 works and results appear to be in good agreement with station-based snowfall measurements (e.g.,

428 Zubler et al., 2014). The coarse grid (12 km) reference snowfall  $S_{SG}$  is determined by averaging the  
 429 sum of separated daily high resolution  $S'$  over all  $n$  high-resolution grid points  $i$  located within a specific  
 430 coarse grid point  $k$ . I.e., at each coarse grid point  $k$

$$431 \quad S_{SG} = \frac{1}{n} \cdot \sum_{i=1}^n P'_i [T'_i \leq T^*] = \frac{1}{n} \sum_{i=1}^n S'_i \quad (3)$$

432 For comparison, the same binary fractionation method with a temperature threshold of  $T^*=2^\circ\text{C}$  is  
 433 directly applied on the coarse 12 km grid (*Binary method*). For this purpose, total precipitation  $P'$  and  
 434 daily mean temperature  $T'$  of the high-resolution data are conservatively remapped to the coarse grid  
 435 leading to  $P$  and  $T$ , respectively. Compared to the *Subgrid method*, the *Binary method* neglects any  
 436 subgrid-scale variability of the snowfall fraction. As a result, the *Binary method* underestimates  $S_{\text{mean}}$   
 437 and overestimates  $S_{\text{q99}}$  for most elevation intervals (Fig. 2). The underestimation of  $S_{\text{mean}}$  can be  
 438 explained by the fact that even for a coarse grid temperature above  $T^*$  individual high-elevation  
 439 subgrid cells (at which  $T \leq T^*$ ) can receive substantial snowfall amounts. As positive precipitation-  
 440 elevation gradients can be assumed for most parts of the domain (larger total precipitation at high  
 441 elevations; see e.g. Kotlarski et al., 2012 and Kotlarski et al., 2015 for an Alpine-scale assessment)  
 442 the neglect of subgrid-scale snowfall variation in the *Binary method* hence leads to a systematic  
 443 underestimation of mean snowfall compared to the *Subgrid method*. Furthermore, following O'Gorman  
 444 (2014), heavy snowfall events are expected to occur in a narrow temperature range below the rain-  
 445 snow transition. As the *Binary method* in these temperature ranges always leads to a snowfall fraction  
 446 of 100%, too large  $S_{\text{q99}}$  values would result.

447 To take into account these subgrid-scale effects, a more sophisticated approach – referred to as the  
 448 *Richards method* – is developed here. This method is based upon a generalised logistic regression  
 449 (Richards, 1959). Here, we apply this regression to relate the surface temperature  $T$  to the snow  
 450 fraction  $f_s$  by accounting for the topographic subgrid-scale variability. At each coarse grid-point  $k$ , the  
 451 *Richards method*-based snowfall fraction  $f_{s,RI}$  for a given day is hence computed as follows:

$$452 \quad f_{s,RI}(T_k) = \frac{1}{[1 + C_k e^{D_k(T_k - T^*)}]^{1/C_k}} \quad (4)$$

453 with  $C$  as the point of inflexion (denoting the point with largest slope), and  $D$  the growth rate (reflecting  
 454 the mean slope).  $T_k$  is the daily mean temperature of the corresponding coarse grid box  $k$  and  $T^*=2^\circ\text{C}$   
 455 the snow fractionation temperature. First, we estimate the two parameters  $C$  and  $D$  of Equation 4 for  
 456 each single coarse grid point  $k$  by minimizing the least-square distance to the  $f_s$  values derived by the  
 457 *Subgrid method* via the reference snowfall  $S_{SG}$  (local fit). Second,  $C$  and  $D$  are expressed as a function  
 458 of the topographic standard deviation  $\sigma_h$  of the corresponding coarse resolution grid point only (Fig.  
 459 S1; global fit). This makes it possible to define empirical functions for both  $C$  and  $D$  that can be used  
 460 for all grid points  $k$  in the Alpine domain and that depend on  $\sigma_h$  only.

$$461 \quad \sigma_{h,k} = \sqrt{\frac{\sum_i^n (h_i - \bar{h}_k)^2}{n-1}} \quad (5)$$

$$462 \quad C_k = \frac{1}{(E - \sigma_{h,k} \cdot F)} \quad (6)$$

463  $D_k = G \cdot \sigma_{h,k}^{-H}$  (7)

464 Through a minimisation of the least square differences the constant parameters in Equations 6 and 7  
465 are calibrated over the domain of Switzerland and using daily data from the period September to May  
466 1971-2005 leading to values of  $E=1.148336$ ,  $F=0.000966 \text{ m}^{-1}$ ,  $G=143.84113 \text{ }^\circ\text{C}^{-1}$  and  $H=0.8769335$ .  
467 Note that  $\sigma_h$  is sensitive to the resolution of the two grids to be compared (cf. Eq. 5). It is a measure for  
468 the uniformity of the underlying topography and has been computed based on the high-resolution  
469 GTOPO30 digital elevation model (<https://lta.cr.usgs.gov/GTOPO30>) aggregated to a regular grid of  
470 1.25 arc seconds (about 2 km) which reflects the spatial resolution of the observed temperature and  
471 precipitation grids (cf. Section 2.1). Small values of  $\sigma_h$  indicate a low subgrid-scale topographic  
472 variability, such as in the Swiss low-lands, while high values result from non-uniform elevation  
473 distributions, such as in areas of inner Alpine valleys.  $\sigma_h$  as derived from GTOPO30 might be different  
474 from the subgrid-scale topographic variance employed by the climate models themselves, which is  
475 however not relevant here as only grid cell-averaged model output is analysed ~~and as we consider~~  
476 ~~while  $\sigma_h$  is regarded~~ as a proper estimate of subgrid-scale variability.

477 Figure S1 (panel c) provides an example of the relation between daily mean temperature and daily  
478 snow fraction  $f_s$  for grid cells with topographical standard deviations of 50 m and 500 m, respectively.  
479 The snowfall amount  $S_{RI}$  for a particular day and a particular coarse grid box is finally obtained by  
480 multiplying the corresponding  $f_{s,RI}$  and  $P$  values. A comparison with the *Subgrid method* yields very  
481 similar results. For both indices  $S_{\text{mean}}$  and  $S_{\text{q99}}$ , mean ratios across all elevation intervals are close to 1  
482 (Fig. 2). At single grid points, maximum deviations are not larger than  $1\pm 0.1$ . Note that for this  
483 comparison calibration and validation period are identical (EVAL period). Based on this analysis, it has  
484 been decided to separate snowfall according to the *Richards method* throughout this work in both the  
485 observations and in the RCMs. The observation-based snowfall estimate obtained by applying the  
486 *Richards method* to the observational temperature and precipitation grids after spatial aggregation to  
487 the  $0.11^\circ$  RCM resolution will serve as reference for the RCM bias adjustment and will be termed  
488 *reference* hereafter. One needs to bear in mind that the parameters  $C$  and  $D$  of the Richards method  
489 were fitted for the Swiss domain only and were later on applied to the entire Alpine domain (cf. Fig. 1).

## 490 2.6 Bias adjustment approach

491 Previous work has revealed partly substantial temperature and precipitation biases of the EURO-  
492 CORDEX RCMs over the Alps (e.g. Kotlarski et al., 2014; Smiatek et al., 2016), and one has to expect  
493 that the separated snowfall amounts are biased too. This would especially hamper the interpretation of  
494 absolute climate change signals of the considered snow indices. We therefore explore possibilities to  
495 bias-adjust the simulated snowfall amounts and to directly integrate this bias adjustment into the  
496 snowfall separation framework of Section 2.5. Note that we deliberately employ the term *bias*  
497 *adjustment* as opposed to *bias correction* to make clear that only certain aspects of the snowfall  
498 climate are adjusted and that the resulting dataset might be subject to remaining inaccuracies.

499 A simple two-step approach that separately accounts for precipitation and temperature biases and  
500 their respective influence on snowfall is chosen. The separate consideration of temperature and

501 precipitation biases allows for a more physically-based bias adjustment of snowfall amounts: Due to  
502 the temperature dependency of snowfall occurrence, snowfall biases of a given climate model cannot  
503 be expected to remain constant under ~~current and future changing~~(i.e., warmer) climate conditions.  
504 For instance, a climate model with a given temperature bias might pass the snow-rain temperature  
505 threshold earlier or later than reality during the general warming process. Hence, traditional bias  
506 adjustment approaches based only on a comparison of observed and simulated snowfall amounts in  
507 the historical climate would possibly fail due to a non-stationary bias structure. The bias adjustment is  
508 calibrated in the EVAL period for each individual GCM-RCM chain and over the region of Switzerland,  
509 and is then applied to both the CTRL and SCEN period of each chain and for the entire Alpine domain.  
510 To be consistent in terms of horizontal grid spacing, the observational data sets RhiresD and TabsD  
511 (see Sec. 2.1) are conservatively regridded to the RCM resolution beforehand.

512 In a first step, total simulated precipitation was adjusted by introducing an elevation-dependent  
513 adjustment factor which adjusts precipitation biases regardless of temperature. For this purpose, mean  
514 precipitation ratios (RCM simulation divided by observational analysis) for 250 m elevation intervals  
515 were calculated (Fig. S32). An almost linear relationship of these ratios with elevation was found.  
516 Thus, a linear regression between the intervals from 250 m a.s.l. to 2750 m a.s.l. was used for each  
517 model chain separately to estimate a robust adjustment factor. As the number of both RCM grid points  
518 and measurement stations at very high elevations (>2750 m a.s.l.) is small (~~see~~ Sec. 2.1; Fig. S2) and  
519 biases are subject to a considerable sampling uncertainty, these elevations were not considered in the  
520 regression. Overall the fits are surprisingly precise except for the altitude bins above 2000 m (Fig.  
521 S32). The precipitation adjustment factors ( $P_{AF}$ ) for a given elevation were then obtained as the  
522 inverse of the fitted precipitation ratios. Multiplying simulated precipitation  $P$  with  $P_{AF}$  for the respective  
523 model chain and elevation results in the adjusted precipitation:

$$524 \quad P_{adj} = P \cdot P_{AF} \quad (8)$$

525 For a given GCM-RCM chain and for each elevation interval, the spatially and temporally averaged  
526 corrected total precipitation  $P_{adj}$  approximately corresponds to the observation-based estimate in the  
527 EVAL period.

528 In the second step of the bias adjustment procedure, temperature biases are accounted for. For this  
529 purpose the initial snow fractionation temperature  $T^*=2^\circ\text{C}$  of the Richards separation method (see Sec  
530 2.5) is shifted to the value  $T_a^*$  for which the spatially (Swiss domain) and temporally (September to  
531 May) averaged simulated snowfall amounts for elevations below 2750 m a.s.l. match the respective  
532 observation-based reference (see above). Compared to the adjustment of total precipitation,  $T_a^*$  is  
533 chosen independent of elevation but separately for each GCM-RCM chain, in order to avoid over-  
534 parameterization and to not over-interpret the elevation dependency of mean snowfall in the snowfall  
535 reference grid. After this second step of the bias adjustment, the spatially and temporally-  
536 simulated snowfall amounts below 2750 m a.s.l. match the reference by definition. Hence, the  
537 employed simple bias adjustment procedure adjusts domain-mean snowfall biases averaged over the  
538 entire season from September to May. It does, however, not correct for biases in the spatial snowfall  
539 pattern, in the seasonal cycle, or in the temporal distribution of daily values. Note that, as the

540 underlying high-resolution data sets are available over Switzerland only, the calibration of the bias  
541 adjustment methodology is correspondingly restricted, but the adjustment is then applied to the whole  
542 Alpine domain. This approach is justified as elevation-dependent mean winter precipitation and  
543 temperature biases of the RCMs employed – assessed by comparison against the coarser-resolved  
544 EOBS reference dataset (Haylock et al., 2008) - are very similar for Switzerland and for the entire  
545 Alpine analysis domain (Figs. S43 and S54).

## 546 **3 Evaluation**

### 547 **3.1 RCM raw snowfall**

548 We first carry out an illustrative comparison of RCM raw snowfall amounts (for those simulations only  
549 that directly provide snowfall flux) against station observations of snowfall in order to determine  
550 whether the simulated RCM snowfall climate contains valid information despite systematic biases. To  
551 this end, simulated raw snowfall amounts of ~~seven~~nine EURO-CORDEX simulations (~~see~~-Tab. 1)  
552 averaged over 250 m-elevation intervals and over the range 950 – 1650 m a.s.l. are compared against  
553 observations of measured fresh snow sums from 29 MeteoSwiss stations (~~see~~-Section 2.1).. For this  
554 purpose a mean snow density of 100 kg/m<sup>3</sup> for the conversion from measured snow depth to water  
555 equivalent is assumed. Note that this simple validation is subject to considerable uncertainties as it  
556 does not explicitly correct for the scale and elevation gap between grid-cell based RCM output and  
557 single-site observations. Especially in complex terrain and for exposed sites, point measurements of  
558 snow depth might be non-representative for larger-scale conditions (e.g., Grünwald and Lehning,  
559 2015). Also, the conversion from snow depth to snow water equivalent is of approximate nature only,  
560 and fresh snow sums might furthermore misrepresent true snowfall in case that snow melt or snow  
561 drift occurs between two snow depth readings.

562 At low elevations simulated mean September-May raw snowfall sums match the observations well  
563 while differences are larger aloft (Fig. 3a). The positive bias at high elevations might arise from the fact  
564 that (the very few) observations were made at specific locations while simulated grid point values of  
565 the corresponding elevation interval might be located in different areas of Switzerland. It might also be  
566 explained by positive RCM precipitation and negative RCM temperature biases at high elevations of  
567 the Alps (e.g., Kotlarski et al., 2015). Also note that, in general, the total high-elevation area of the  
568 Alpine analysis domain is small and elevations above 2500 m represent less than 5% of the total area  
569 (Fig. S2). Both model-based and observation-based estimates for high-elevations are hence subject to  
570 a considerable sampling uncertainty and are likely to be less robust than estimates for lower  
571 elevations.

572 At lower elevations, the station network is geographically more balanced and the observations are  
573 probably more representative of the respective elevation interval. Despite a clear positive snowfall bias  
574 in mid-winter, the RCMs are generally able to reproduce the mean seasonal cycle of snowfall for  
575 elevations between 950 m a.s.l. - 1650 m a.s.l. (Fig. 3b). The fact that the major patterns of both the  
576 snowfall-elevation relationship and the mean seasonal snowfall cycle are well represented indicates  
577 the general and physically consistent applicability of RCM output to assess future changes in mean



578 and heavy Alpine snowfall. However, substantial biases in snowfall amounts are apparent and a bias  
579 adjustment of simulated snowfall seems to be required prior to the analysis of climate change signals  
580 of individual snowfall indices.

### 581 **3.2 Evaluation of the reference snowfall**

582 The snowfall separation employing the *Richards method* (Section 2.5) and, as a consequence, also  
583 the bias adjustment (Section 2.6) make use of the 2 km reference snowfall grid derived by employing  
584 the *Subgrid method* on the observed temperature and precipitation grids. Hence, the final results of  
585 this study could to some extent be influenced by inaccuracies and uncertainties of the reference  
586 snowfall grid itself. In order to assess the quality of the latter and in absence of a further observation-  
587 based reference we here present an approximate evaluation.

588 First, the reference snowfall grid is evaluated against fresh snow sums at the 29 Swiss stations that  
589 were also used for evaluating RCM raw snowfall. Note the limitations of such a comparison as outlined  
590 in Chapter 3.1. The comparison of black and red markers and lines in Figure 3 indicates a good  
591 agreement of mean snowfall at individual elevation intervals (left panel) as well for the mean annual  
592 cycle of snowfall at medium elevations (right panel). The reference snowfall grid is obviously a good  
593 approximation of site-scale fresh snow sums. Note that similarly to the RCM raw snowfall evaluation,  
594 all 2 km reference snowfall grid cells in the respective elevation interval are considered. The good  
595 agreement, however, still holds if only those 2 km grid cells covering the 29 site locations are  
596 considered (not shown here).

597 Second, both the 2 km reference snowfall grid and the 0.11° reference snowfall grid obtained by  
598 employing the Richards method to aggregated temperature and precipitation values (see Section 2.5)  
599 are compared against the gridded HISTALP dataset of solid precipitation (Chimani et al., 2011). The  
600 latter is provided at a monthly resolution on a 5' grid covering the Greater Alpine Region. It is based on  
601 monthly snowfall fraction estimates that are used to scale a gridded dataset of total precipitation. The  
602 comparison of the three datasets for the region of Switzerland (for which the 2 km reference snowfall  
603 is available) in the EVAL period 1971-2005 yields an approximate agreement of both the magnitude of  
604 mean winter snowfall and its spatial pattern (Fig. S6). The three data sets differ with respect to their  
605 spatial resolution but all show a clear dependency of snowfall on topography and mean September-  
606 May snowfall sums above 1000 mm over most parts of the Alpine ridge. Climatologically warm and dry  
607 valleys, on the other hand, are represented by minor snowfall amounts of less than 400 mm only.

608 As mentioned before these evaluations of the reference snowfall grid are subject to uncertainties and,  
609 furthermore, they only cover mean snowfall amounts. However, they provide basic confidence in the  
610 applicability of the reference snowfall grid for the purposes of snowfall separation and bias adjustment  
611 in the frame of the present study.

612



### 613 3.3 Calibration of bias adjustment

614 The analysis of total precipitation ratios (RCM simulations with respect to observations) for the EVAL  
615 period, which are computed to carry out the first step of the bias adjustment procedure, reveals  
616 substantial elevation dependencies. All simulations tend to overestimate total precipitation at high  
617 elevations (Fig. S32). This fact might ultimately be connected to an overestimation of surface snow  
618 amount in several EURO-CORDEX RCMs as reported by Terzago et al. (2017). As the precipitation  
619 ratio between simulations and observations depends approximately linearly on elevation, the  
620 calculation of  $P_{AF}$  via a linear regression of the ratios against elevation (see Sec. 2.6) seems  
621 reasonable. By taking the inverse of this linear relation,  $P_{AF}$  for every model and elevation can be  
622 derived. For the CCLM and RACMO-simulations, these correction factors do not vary much with  
623 height, while  $P_{AF}$  for MPI-ESM - REMO and EC-EARTH - HIRHAM is much larger than 1 in low lying  
624 areas, indicating a substantial underestimation of observed precipitation sums (Fig. 4a). However, for  
625 most elevations and simulations,  $P_{AF}$  is generally smaller than 1, i.e., total precipitation is  
626 overestimated by the models. Similar model biases in the winter and spring seasons have already  
627 been reported in previous works (e.g., Rajczak et al., in-prep-2017; Smiatek et al., 2016). Especially at  
628 high elevations, these apparent positive precipitation biases could be related to observational  
629 undercatch, i.e., an underestimation of true precipitation sums by the observational analysis. Frei et al.  
630 (2003) estimated seasonal Alpine precipitation undercatch for three elevation intervals. Results show  
631 that measurement biases are largest in winter and increase with altitude. However, a potential  
632 undercatch (with a maximum of around 40% at high elevations in winter; Frei et al., 2003) can only  
633 partly explain the often partly-substantial overestimation of precipitation found in the present work.

634 After applying  $P_{AF}$  to the daily precipitation fields, a snowfall fractionation at the initial  $T^*$  of 2 °C (see  
635 Eq. (4)) would lead to a snowfall excess in all 124 simulations as models typically experience a cold  
636 winter temperature bias. To match the observation-based and spatio-temporally averaged reference  
637 snowfall below 2750 m a.s.l.,  $T^*$  for all models needs to be decreased during the second step of the  
638 bias adjustment (Fig. 4b). The adjusted  $T_a^*$  values indicate a clear positive relation with the mean  
639 temperature bias in the EVAL period. This feature is expected since the stronger a particular model's  
640 cold bias the stronger the required adjustment of the snow fractionation temperature  $T^*$  towards lower  
641 values in order to avoid a positive snowfall bias. Various reasons for the scatter around a simple linear  
642 relation in Figure 4b can be thought of. These include remaining spatial inaccuracies of the corrected  
643 precipitation grid, elevation-dependent temperature biases and misrepresented temperature-  
644 precipitation relationships at daily scale. Note that precipitation and temperature biases heavily  
645 depend on the GCM-RCM chain and seem to be rather independent from each other. While EC-  
646 EARTH - RACMO, for instance, shows one of the best performances in terms of total precipitation, its  
647 temperature bias close to -5 °C is the largest deviation in our set of simulations. Concerning the partly  
648 substantial temperature biases of the EURO-CORDEX models shown in Figure 4-b, their magnitude  
649 largely agrees with Kotlarski et al. (2014; in reanalysis-driven simulations) and Smiatek et al. (2016).

650 **3.4 Evaluation of snowfall indices**

651 We next assess the performance of the bias adjustment procedure by comparing snowfall indices  
652 derived from separated and bias-adjusted RCM snowfall amounts against the observation-based  
653 reference. The period for which this comparison is carried out is EVAL, i.e., it is identical to the  
654 calibration period of the bias adjustment. We hence do not intend a classical cross validation exercise  
655 with separate calibration and validation periods, but try to answer the following two questions: (a)  
656 Which aspects of the Alpine snowfall climate are adjusted, and (b) for which aspects do biases remain  
657 even after application of the bias adjustment procedure.

658 Figure 5 shows the evaluation results of the six snowfall indices based on the separated and not bias-  
659 adjusted simulated snowfall ( $RCM_{sep+nba}$ ), and the separated and bias-adjusted simulated snowfall  
660 ( $RCM_{sep+ba}$ ). In the first case the snowfall separation of raw precipitation is performed with  $T^* = -2^\circ\text{C}$ ,  
661 while in the second case precipitation is adjusted and the separation is performed with a bias-adjusted  
662 temperature  $T^*_a$ . The first column represents the mean September to May statistics, while columns 2-4  
663 depict the seasonal cycle at monthly resolution for three distinct elevation intervals.

664 The analysis of  $S_{mean}$  confirms that  $RCM_{sep+ba}$  is able to reproduce the observation-based reference in  
665 the domain mean as well as in most individual elevation intervals. The domain-mean agreement is a  
666 direct consequence of the design of the bias adjustment procedure (see above).  $RCM_{sep+nba}$ , on the  
667 other hand, consistently overestimates  $S_{mean}$  by up to a factor of 2.5 as a consequence of positive  
668 precipitation and negative temperature biases (cf. Fig. 4). Also the seasonal cycle of  $S_{mean}$  for  
669  $RCM_{sep+ba}$  yields a satisfying performance across all three elevation intervals, while  $RCM_{sep+nba}$  tends  
670 to produce too much snowfall over all months and reveals an increasing model spread with elevation.

671 For the full domain and elevations around 1000 m, the observation-based reference indicates a mean  
672  $S_{freq}$  of 20% between September and May. Up to 1000 m a.s.l.  $RCM_{sep+ba}$  reflects the increase of this  
673 index with elevation adequately. However, towards higher elevations the approximately constant  $S_{freq}$   
674 of 30% in the reference is not captured by the simulation-derived snowfall. Notably during wintertime,  
675 both  $RCM_{sep+ba}$  and  $-RCM_{sep+nba}$  produce too many snowfall days, i.e., overestimate snowfall  
676 frequency. This feature is related to the fact that climate models typically tend to overestimate the wet  
677 day frequency over the Alps especially in wintertime (Rajczak et al., 2013) and that the bias  
678 adjustment procedure employed does not explicitly correct for potential biases in precipitation  
679 frequency. Due to the link between mean snowfall on one side and snowfall frequency and mean  
680 intensity on the other side, opposite results are obtained for the mean snowfall intensity  $S_{int}$ .  $RCM_{sep+ba}$   
681 largely underestimates mean intensities during snowfall days while  $RCM_{sep+nba}$  typically better reflects  
682 the reference. Nevertheless, deviations during winter months at mid-elevations are not negligible.  
683 Mean September-May  $S_{frac}$  in the reference exponentially increases with elevation. This behaviour is  
684 reproduced by both  $RCM_{sep+ba}$  and  $RCM_{sep+nba}$ . Notwithstanding,  $RCM_{sep+ba}$  results are more accurate  
685 compared to  $RCM_{sep+nba}$ , which turns out to be biased towards too large snowfall fractions.

686 For the two heavy snowfall indices  $S_{q99}$  and  $S_{1d}$ ,  $RCM_{sep+nba}$  appears to typically match the reference  
687 better than  $RCM_{sep+ba}$ . Especially at high elevations,  $-RCM_{sep+ba}$  produces too low snowfall amounts.

688 This again illustrates the fact that the bias adjustment procedure is designed to adjust biases in mean  
689 snowfall, but does not necessarily improve further aspects of the simulated snowfall climate.

690 The spatial patterns of  $S_{\text{mean}}$  for the 124 RCM<sub>sep+ba</sub> simulations from September to May are presented  
691 in Figure 6. The observational-based reference (~~lower-right-bottom~~ panel) reveals a snowfall  
692 distribution with highest values along the Alpine main ridge, whereas the Swiss plateau, Southern  
693 Ticino and main valleys such as the Rhône and Rhine valley experience less snowfall. Almost all bias-  
694 adjusted models are able to represent the overall picture with snow-poor lowlands and snow-rich  
695 Alpine regions. Nevertheless substantial differences to the observations concerning the spatial  
696 snowfall pattern can arise. EC-EARTH - HIRHAM, for example, is subject to a "pixelated"noisy  
697 structure. This could be the result of frequent grid-cell storms connected to parameterisations  
698 struggling with complex topographies. Such inaccuracies in the spatial pattern are not corrected for by  
699 our simple bias adjustment approach which only targets domain-mean snowfall amounts at elevations  
700 below 2750 m a.s.l. and that does not considerably modify the simulated spatial snowfall patterns..  
701 Note that these patterns are obviously strongly determined by the RCM itself and only slightly depend  
702 on the driving GCM (see, for instance, the good agreement among the CCLM and the RCA  
703 simulations).

704 In summary, after applying the bias adjustment to the simulations most snowfall indices are fairly well  
705 represented at elevations below 1000 m a.s.l.. With increasing altitude and smaller sample sizes in  
706 terms of number of grid cells, reference and RCM<sub>sep+ba</sub> diverge. This might be caused by the remaining  
707 simulated overestimation of  $S_{\text{freq}}$  and an underestimation of  $S_{\text{int}}$ . While the bias adjustment approach  
708 leads to a reduction of  $S_{\text{int}}$  due to the total precipitation adjustment,  $S_{\text{freq}}$  is only slightly modified by this  
709 correction and by the adjustment of  $T^*$ . Nevertheless, these two parameters strongly influence other  
710 snowfall indices. The counteracting effects of overestimated  $S_{\text{freq}}$  and underestimated  $S_{\text{int}}$  result in  
711 appropriate amounts of  $S_{\text{mean}}$  whereas discrepancies for  $S_{\text{q99}}$  and  $S_{\text{1d}}$  are mainly driven by the  
712 underestimation of  $S_{\text{int}}$ .

#### 713 **4 Snowfall projections for the late 21<sup>st</sup> century**

714 For the study of climate change signals, the analysis domain is extended to the entire Alps (see Sec.  
715 2.3). Due to the identified difficulties of bias-adjusting certain snowfall indices (see Sec 3.4), emphasis  
716 is laid upon relative signals of change (see Eq. 2). This type of change can be expected to be less  
717 dependent on the remaining inaccuracies after the adjustment. If not stated otherwise, all results in  
718 this Section are based on the RCM<sub>sep+ba</sub> data, i.e., on separated and bias-adjusted RCM snowfall, and  
719 on the RCP8.5 emission scenario.

720 Projections for seasonal  $S_{\text{mean}}$  show a considerable decrease over the entire Alpine domain (Fig. 7).  
721 Most RCMs project largest percentage losses of more than 80% across the Alpine forelands and  
722 especially in its topographic depressions such as the Po and Rhone valleys. Over the Alpine ridge,  
723 reductions are smaller but still mostly negative. Elevated regions between Southeastern Switzerland,  
724 Northern Italy and Austria seem to be least affected by the overall snowfall reduction. Some of the  
725 simulations (e.g., CNRM-RCA, -MPI-ESM-RCA or MPI-ESM-REMO) project only minor changes in

726 these regions. Experiments employing the same RCM but different driving GCMs (e.g. the four  
727 simulations of RCA), but also experiments employing the same GCM but different RCMs (e.g. the ~~four~~  
728 three simulations driven by EC-EARTH, though different realizations) can significantly disagree in  
729 regional-scale change patterns and especially in the general magnitude of change. This highlights a  
730 strong influence of both the driving GCMs and the RCMs themselves on snowfall changes,  
731 representing effects of large-scale circulation and meso-scale response, respectively.

732 A more detailed analysis is provided in Fig. 8 which addresses the vertical and seasonal distribution of  
733 snowfall changes. It reveals that relative (seasonal mean) changes of  $S_{\text{mean}}$  appear to be strongly  
734 dependent on elevation (Fig.8, top left panel). The multi-model mean change ranges from -80% at low  
735 elevations to -10% above 3000 m a.s.l.. Largest differences between neighbouring elevation intervals  
736 are obtained from 750 m a.s.l. to 1500 m a.s.l.. Over the entire Alps, the results show a reduction of  
737  $S_{\text{mean}}$  by -35% to -55% with a multi-model mean of -45%. The multi-model spread appears to be rather  
738 independent of elevation and is comparably small, confirming that, overall, the spatial distributions of  
739 the change patterns are similar across all model chains (cf. Fig. 7). All simulations point to decreases  
740 over the entire nine-month period September to May for the two elevation intervals <1000 m a.s.l. and  
741 1000 to 2000 m a.s.l.. Above 2000 m a.s.l., individual simulations show an increase of  $S_{\text{mean}}$  by up to  
742 20% in mid-winter which leads to a slightly positive change in multi-model mean in January and  
743 February.

744 Decreases of  $S_{\text{freq}}$  are very similar to changes in mean snowfall. Mean September-May changes are  
745 largest below 1000 m a.s.l., while differences among elevation intervals become smaller at higher  
746 elevations. In-between is a transition zone with rather strong changes with elevation, which  
747 approximately corresponds to the mean elevation of the September-May zero-degree line in today's  
748 climate (e.g., Ceppi et al., 2012; MeteoSchweiz, 2016). Individual simulations with large reductions in  
749  $S_{\text{mean}}$ , such as the RCA experiments, also project strongest declines in  $S_{\text{freq}}$ . In contrast, the mean  
750 snowfall intensity  $S_{\text{int}}$  is subject to smallest percentage variations in our set of snowfall indices. Strong  
751 percentage changes for some models in September are due to the small sample size (only few grid  
752 points considered) and the low snowfall amounts in this month. Apart from mid elevations with  
753 decreases of roughly -10%, mean intensities from September to May are projected to remain almost  
754 unchanged by the end of the century. For both seasonal and monthly changes, model agreement is  
755 best for high elevations while the multi-model spread is largest for lowlands. Large model spread at  
756 low elevations might be caused by the small number of grid points used for averaging over the  
757 respective elevation interval, especially in autumn and spring.

758 Similar results are obtained for the heavy snowfall indices  $S_{\text{q99}}$  and  $S_{\text{1d}}$ . While percentage decreases  
759 at lowermost elevations are even larger than for  $S_{\text{mean}}$ , losses at high elevations are less pronounced,  
760 resulting in similar domain-mean change signals for heavy and mean snowfall. Substantial differences  
761 between monthly  $\delta S_{\text{q99}}$  and  $\delta S_{\text{1d}}$  appear at elevations below 1000 m a.s.l.. Here, percentage losses of  
762  $S_{\text{q99}}$  are typically slightly more pronounced. Above 2000 m a.s.l. both indices appear to remain almost  
763 constant between January and March with change signals close to zero. The multi-model mean  
764 changes even hint to slight increases of both indices. Concerning changes in the snowfall fraction, i.e.,

765 in the relative contribution of snowfall to total precipitation, our results indicate that current seasonal  
766 and domain mean  $S_{frac}$  might drop by about -50% (Fig. 8, lowermost row). Below 1000 m a.s.l., the  
767 strength of the signal is almost independent of the month, and multi-model average changes of the  
768 snow fraction of about -80% are obtained. At higher elevations changes during mid-winter are less  
769 pronounced compared to autumn and spring but still negative.

## 770 5 Discussion

### 771 5.1 Effect of temperature, snowfall frequency and intensity on snowfall changes

772 The results in Section 4 indicate substantial changes of snowfall indices over the Alps in regional  
773 climate projections. With complementary analyses presented in Figures 9 and 10 we shed more light  
774 on the responsible mechanisms, especially concerning projected changes in mean and heavy  
775 snowfall. For this purpose Figures 9a-b,e-f show the relationship of both mean and heavy snowfall  
776 amounts in the CTRL period and their respective percentage changes with the climatological CTRL  
777 temperature of the respective (climatological) month, elevation interval and GCM-RCM chain. For  
778 absolute amounts ( $S_{mean}$ ,  $S_{q99}$ ; Fig. 9a,e) a clear negative relation is found, i.e., the higher the CTRL  
779 temperature the lower the snowfall amounts. For  $S_{mean}$  the relation levels off at mean temperatures  
780 higher than about 6°C with mean snowfall amounts close to zero. For temperatures below about -6°C  
781 a considerable spread in snowfall amounts is obtained, i.e., mean temperature does not seem to be  
782 the controlling factor here. Relative changes of both quantities (Fig. 9b,f), however, are strongly  
783 controlled by the CTRL period's temperature level with losses close to 100% for warm climatic settings  
784 and partly increasing snowfall amounts for colder climates. This dependency of relative snowfall  
785 changes on CTRL temperature is in line with previous works addressing future snowfall changes on  
786 both hemispheric and regional scales (de Vries et al., 2014; Krasting et al., 2013; Räisänen, 2016).  
787 The spread of changes within a given CTRL temperature bin can presumably be explained by the  
788 respective warming magnitudes that differ between elevations, months and GCM-RCM chains. About  
789 half of this spread can be attributed to the month and the elevation alone (compare the spread of the  
790 black markers to the one of the red markers which indicate multi-model averages).

791 For most months and elevation intervals, percentage reductions in  $S_{mean}$  and  $S_{q99}$  reveal an almost  
792 linear relationship with  $-\delta S_{freq}$  (Fig. 9c, g). The decrease of  $S_{freq}$  with future warming can be explained  
793 by a shift of the temperature probability distribution towards higher temperatures, leading to fewer  
794 days below the freezing level (Fig. 10, top row). Across the three elevation intervals <1000 m a.s.l.,  
795 1000-2000 m a.s.l. and > 2000 m a.s.l., relative changes in the number of days with temperatures  
796 below the freezing level ( $T \leq 0^\circ\text{C}$ ) are in the order of -65%, -40% and -20%, respectively (not shown).  
797 This approximately corresponds to the simulated decrease of  $S_{freq}$  (cf. Fig 8), which in turn, is of a  
798 similar magnitude as found in previous works addressing future snowfall changes in the Alps  
799 (Schmucki et al., 2015b; Zubler et al., 2014). Due to the general shift of the temperature distribution  
800 and the "loss" of very cold days (Fig. 10, top row) future snowfall furthermore occurs in a narrower  
801 temperature range (Fig. 10, second row).

802 Contrasting this general pattern of frequency-driven decreases of both mean and heavy snowfall, no  
803 changes or even slight increases of  $S_{\text{mean}}$ ,  $S_{\text{q99}}$  and  $S_{1\text{d}}$  at high elevations are expected in mid-winter  
804 (see Fig. 8). This can to some part be explained by the general increase of total winter precipitation  
805 (Rajczak et al., [in-prep2017](#); Smiatek et al., 2016) that obviously offsets the warming effect in high-  
806 elevation regions where a substantial fraction of the future temperature PDF is still located below the  
807 rain-snow transition (Fig. 10, top row). This process has also been identified in previous works to be,  
808 at last partly, responsible for future snowfall increases (de Vries et al., 2014; Krasting et al., 2013;  
809 Räisänen, 2016). Furthermore, the magnitude of the increases of both mean and heavy snowfall is  
810 obviously driven by positive changes of  $S_{\text{int}}$ , while  $S_{\text{freq}}$  remains constant (Fig. 9c,g). An almost linear  
811 relationship between positive changes of  $S_{\text{int}}$  and positive changes of  $S_{\text{mean}}$  and  $S_{\text{q99}}$  is obtained (Fig.  
812 9d,h; upper right quadrants. Nevertheless, the high-elevation mid-winter growth in  $S_{\text{mean}}$  is smaller  
813 than the identified increases of mean winter total precipitation. This can be explained by the persistent  
814 decrease of  $S_{\text{frac}}$  during the cold season (see -Fig. 8, lowermost row).

815 For elevation intervals with simulated monthly temperatures between  $-6^{\circ}\text{C}$  and  $0^{\circ}\text{C}$  in the CTRL  
816 period,  $S_{\text{mean}}$  appears to decrease stronger than  $S_{\text{q99}}$  (cf. Fig. 9b,f). O’Gorman (2014) found a very  
817 similar behaviour when analysing mean and extreme snowfall projections over the Northern  
818 Hemisphere within a set of GCMs. This finding is related to the fact that future snowfall decreases are  
819 mainly governed by a decrease of snowfall frequency while snowfall increases in high-elevated  
820 regions in mid-winter seem to be caused by increases of snowfall intensity. It can obviously be  
821 explained by the insensitivity of the temperature interval at which extreme snowfall occurs to climate  
822 warming and by the shape of the temperature – snowfall intensity distribution itself (Fig. 10, third row).  
823 The likely reason behind positive changes of  $S_{\text{int}}$  at high-elevated and cold regions is the higher water  
824 holding capacity of the atmosphere in a warmer climate. According to the Clausius-Clapeyron relation,  
825 saturation vapour pressure increases by about 7% per degree warming (Held and Soden, 2006).  
826 Previous studies have shown that simulated changes of heavy and extreme precipitation [on daily time](#)  
827 [scales \(though not necessarily targeting the daily temporal scale and moderate extremes as in our](#)  
828 [case\)](#) are consistent with this theory (e.g., Allen and Ingram, 2002; [Ban et al., 2015](#)[Rajczak et al.,](#)  
829 [2017](#)). In terms of snowfall, we find the Clausius-Clapeyron relation to be applicable for negative  
830 temperatures up to approximately  $-5^{\circ}\text{C}$  as well (Fig. 10, third row, dashed lines). Inconsistencies for  
831 temperatures between  $-5^{\circ}\text{C}$  and  $0^{\circ}\text{C}$  are due to a snow fraction  $sf < 100\%$  for corresponding  
832 precipitation events.

833 For further clarification, Figure 11 schematically illustrates the governing processes behind the  
834 changes of mean and heavy snowfall that differ between climatologically warm (decreasing snowfall)  
835 and climatologically cold climates (increasing snowfall). As shown in Figure 10 (third row), the mean  
836  $S_{\text{int}}$  distribution is rather independent on future warming and similar temperatures are associated with  
837 similar mean snowfall intensities. In particular, heaviest snowfall is expected to occur slightly below the  
838 freezing level in both the CTRL and the SCEN period (Fig. 11a). How often do such conditions prevail  
839 in the two periods? In a warm current climate, i.e., at low elevations or in the transition seasons, heavy  
840 snowfall only rarely occurs as the temperature interval for highest snowfall intensity is already situated  
841 in the left tail of the CTRL period’s temperature distribution (Fig. 11b). With future warming, i.e., with a

842 shift of the temperature distribution to the right, the probability for days to occur in the heavy snowfall  
843 temperature interval (dark grey shading) decreases stronger than the probability of days to occur in  
844 the overall snowfall regime (light grey shading). This results in (1) a general decrease of snowfall  
845 frequency, (2) a general decrease of mean snowfall intensity and (3) a general and similar decrease of  
846 both mean and heavy snowfall amounts. In contrast, at cold and high-elevated sites CTRL period  
847 temperatures are often too low to trigger heavy snowfall since a substantial fraction of the temperature  
848 PDF is located to the left of the heavy snowfall temperature interval (Fig. 11 c). The shifted distribution  
849 in a warmer SCEN climate, however, peaks within the temperature interval that favours heavy  
850 snowfall. This leads to a probability increase for days to occur in the heavy snowfall temperature range  
851 despite the general reduction in  $S_{freq}$  (lower overall probability of days to occur in the entire snowfall  
852 regime, light grey). As a consequence, mean  $S_{int}$  tends to increase and the reduction of heavy snowfall  
853 amounts is less pronounced (or even of opposing sign) than the reduction in mean snowfall. For  
854 individual (climatologically cold) regions and seasons, the increase of mean  $S_{int}$  might even  
855 compensate the  $S_{freq}$  decrease, resulting in an increase of both mean and heavy snowfall amounts.  
856 Note that in a strict sense these explanations only hold in the case that the probability of snowfall to  
857 occur at a given temperature does not change considerably between the CTRL and the SCEN period.  
858 This behaviour is approximately found (Fig. 10, bottom row), which presumably indicates only minor  
859 contributions of large scale circulation changes and associated humidity changes on both the  
860 temperature - snowfall frequency and the temperature - snowfall intensity relation.

## 861 **5.2 Emission scenario uncertainty**

862 The projections presented in the previous sections are based on the RCP8.5 emission scenario, but  
863 will depend on the specific scenario considered. To assess this type of uncertainty we here compare  
864 the RCM<sub>sep+ba</sub> simulations for the previously shown RCP8.5 emission scenario against those assuming  
865 the more moderate RCP4.5 scenario. As a general picture, the weaker RCP4.5 scenario is associated  
866 with less pronounced changes of snowfall indices (Fig. 12). Differences in mean seasonal  $\delta S_{mean}$   
867 between the two emission scenarios are most pronounced below 1000 m a.s.l. where percentage  
868 changes for RCP4.5 are about one third smaller than for RCP8.5. At higher elevations, multi-model  
869 mean changes better agree and the multi-model ranges for the two emission scenarios start  
870 overlapping, i.e., individual RCP4.5 experiments can be located in the RCP8.5 multi-model range and  
871 vice versa. Over the entire Alpine domain, about -25% of current snowfall is expected to be lost under  
872 the moderate RCP4.5 emission scenario while a reduction of approximately -45% is projected for  
873 RCP8.5. For seasonal cycles, the difference of  $\delta S_{mean}$  between RCP4.5 and RCP8.5 is similar for  
874 most months and slightly decreases with altitude. Above 2000 m a.s.l., the simulated increase of  $S_{mean}$   
875 appears to be independent of the chosen RCP in January and February, while negative changes  
876 before and after mid-winter are more pronounced for RCP8.5. Alpine domain mean  $\delta S_{q99}$  almost  
877 doubles under the assumption of stronger GHG emissions. This is mainly due to differences at low  
878 elevations whereas above 2000 m a.s.l.  $\delta S_{q99}$  does not seem to be strongly affected by the choice of  
879 the emission scenario. Differences in monthly mean changes are in close analogy to  $\delta S_{mean}$ . Higher  
880 emissions lead to a further negative shift in  $\delta S_{q99}$ . Up to mid-elevations differences are rather



881 independent of the season. However, at highest elevations and from January to March, differences  
882 between RCP4.5 and RCP8.5 are very small.

883 Despite the close agreement of mid-winter snowfall increases at high elevations between the two  
884 emission scenarios, obvious differences in the spatial extent of the region of mean seasonal snowfall  
885 increases can be found (cf Figs. S76 and 7 for  $\delta S_{\text{mean}}$ , and Figs. S87 and S98 for  $\delta S_{\text{q99}}$ ). In most  
886 simulations, the number of grid cells along the main Alpine ridge that show either little change or even  
887 increases of seasonal mean  $S_{\text{mean}}$  or  $S_{\text{q99}}$  is larger for RCP4.5 than for RCP8.5 with its larger warming  
888 magnitude.

### 889 5.3 Intercomparison of projections with separated and raw snowfall

890 The snowfall projections presented above are based on the RCM<sub>sep+ba</sub> data set, i.e. on separated and  
891 bias-adjusted snowfall amounts. To assess the robustness of these estimates we here compare the  
892 obtained change signals against the respective signals based on RCM<sub>sep+nba</sub> (separated and not bias-  
893 adjusted) and simulated raw snowfall output (RCM<sub>raw</sub>). This comparison is restricted to the ~~nine~~-seven  
894 RCMs providing raw snowfall as output variable (see Tab. 1).

895 The three different change estimates agree well with each other in terms of relative snowfall change  
896 signals (Fig. 13, top row). Multi-model mean relative changes are very similar for all analysed snowfall  
897 indices and elevation intervals. In many cases, separated and not bias-adjusted snowfall (RCM<sub>sep+nba</sub>)  
898 is subject to slightly smaller percentage decreases. Multi-model mean differences between RCM<sub>sep+ba</sub>,  
899 RCM<sub>sep+nba</sub> and RCM<sub>raw</sub> simulations are smaller than the corresponding multi-model spread of  
900 RCM<sub>sep+ba</sub> simulations and emission scenario uncertainties (cf. Figs. 12, 13 and S10). This agreement  
901 in terms of relative change signals is in contrast to absolute change characteristics (Fig. 13, bottom  
902 row). Results based on the three data sets agree in the sign of change, but not in their magnitude,  
903 especially at high elevations >2000 m a.s.l.. As the relative changes are almost identical, the absolute  
904 changes strongly depend upon the treatment of biases in the control climate.

905 In summary, these findings indicate that (a) the snowfall separation method developed in the present  
906 work yields rather good proxies for relative changes of snowfall indices in raw RCM output (which is  
907 not available for all GCM-RCM chains), and that (b) the additional bias adjustment of separated  
908 snowfall amounts only has a weak influence on relative change signals of snowfall indices, but can  
909 have substantial effects on absolute changes.

## 910 6 Conclusions and outlook

911 The present work makes use of state-of-the-art EURO-CORDEX RCM simulations to assess changes  
912 of snowfall indices over the European Alps by the end of the 21st century. For this purpose, snowfall is  
913 separated from total precipitation using near-surface air temperature in both the RCMs and in the ~~an~~  
914 observation-based estimate on a daily basis. The analysis yields a number of robust signals,  
915 consistent across a range of climate model chains and across emission scenarios. Relating to the  
916 main objectives we find the following:



917 | **Snowfall separation on ~~thean~~ RCM grid.** Binary snow fractionation with a fixed temperature  
918 threshold on coarse-resolution grids (with 11 km resolution) leads to an underestimation of mean  
919 snowfall and an overestimation of heavy snowfall. To overcome these deficiencies, the Richards snow  
920 fractionation method is implemented. This approach expresses that the coarse-grid snow fraction  
921 depends not only on daily mean temperature, but also on topographical subgrid-scale variations.  
922 Accounting for the latter results in better estimates for mean and heavy snowfall. However, due to  
923 limited observational coverage the parameters of this method are fitted for Switzerland only and are  
924 then applied to the entire Alpine domain. Whether this spatial transfer is robust could further be  
925 investigated by using observational data sets covering the full domain of interest but is out of the  
926 scope of this study.

927 | **Snowfall bias adjustment.** Simulations of the current EURO-CORDEX ensemble are subject to  
928 considerable biases in precipitation and temperature, which translate into biased snowfall amounts. In  
929 the EVAL period, simulated precipitation is largely overestimated, with increasing biases toward higher  
930 altitudes. On the other hand, simulated near surface temperatures are generally too low with largest  
931 deviations over mountainous regions. These findings were already reported in previous studies for  
932 both the current EURO-CORDEX data set but also for previous RCM ensembles (e.g. Frei et al., 2003;  
933 Kotlarski et al., 2012; Kotlarski et al., 2015; Rajczak et al., 2013; Smiatek et al., 2016). By  
934 implementing a simple bias adjustment approach, we are able to partly reduce these biases and the  
935 associated model spread, which should enable more robust change estimates. The adjusted model  
936 results reproduce the seasonal cycles of mean snowfall fairly well. However, substantial biases remain  
937 in terms of heavy snowfall, snowfall intensities (which in general are overestimated), snowfall  
938 frequencies, and spatial snowfall distributions. Further improvements might be feasible by using more  
939 sophisticated bias adjustment methods, such as quantile mapping (e.g., Rajczak et al., 2016), local  
940 intensity scaling of precipitation (e.g., Schmidli et al., 2006), or weather generators (e.g. Keller et al.,  
941 2016). Advantages of the approach employed here are its simplicity, its direct linkage to the snowfall  
942 separation method and, as a consequence, its potential ability to account for non-stationary snowfall  
943 | biases. Furthermore, a comparison to simulated raw snowfall for a subset of ~~nine-seven~~ simulations  
944 revealed that relative change signals are almost independent of the chosen post-processing strategy.

945 | **Snowfall projections for the late 21st century.** Snowfall climate change signals are assessed by  
946 deriving the changes in snowfall indices between the CTRL period 1981 - 2010 and the SCEN period  
947 2070 - 2099. Our results show that by the end of the 21st century, snowfall over the Alps will be  
948 | considerably reduced. -Between September and May mean snowfall is expected to decrease by  
949 approximately -45% (multi-model mean) under an RCP8.5 emission scenario. For the more moderate  
950 RCP4.5 scenario, multi-model mean projections show a decline of -25%. These results are in good  
951 agreement with previous works (e.g. de Vries et al., 2014; Piazza et al., 2014, Räisänen, 2016). Low-  
952 lying areas experience the largest percentage changes of more than -80%, while the highest Alpine  
953 regions are only weakly affected. Variations of heavy snowfall, defined by the 99% all-day snowfall  
954 percentile, show an even more pronounced signal at low-lying elevations. With increasing elevation,  
955 percentage changes of heavy snowfall are generally smaller than for mean snowfall. O'Gorman (2014)  
956 found a very similar behaviour by analysing projected changes in mean and extreme snowfall over the

957 entire Northern Hemisphere. He pointed out that heavy and extreme snowfall occurs near an optimal  
958 temperature (near or below freezing, but not too cold), which seems to be independent of climate  
959 warming. We here confirm this finding. At mid and high elevations heavy snowfall in a warmer climate  
960 will still occur in the optimal temperature range, hence, heavy snowfall amounts will decrease less  
961 strongly compared to mean snowfall, and may even increase in some areas.

962 At first approximation, the magnitude of future warming strongly influences the reduction of mean and  
963 heavy snowfall by modifying the snowfall frequency. Snowfall increases may however occur at high  
964 (and thus cold) elevations, and these are not caused by frequency changes. Here, snowfall increases  
965 due to (a) a general increase of total winter precipitation combined with only minor changes in snowfall  
966 frequency, and (b) more intense snowfall. This effect has a pronounced altitudinal distribution and may  
967 be particularly strong under conditions (depending upon location and season) where the current  
968 climate is well below freezing. ~~Such conditions may experience~~With the expected warming a shift  
969 towards a temperature range more favourable to snowfall (near or below freezing, but not too cold)  
970 can be expected with corresponding increases of mean snowfall, despite a general decrease of the  
971 snowfall fraction.

972 The identified future changes of snowfall over the Alps can lead to a variety of impacts in different  
973 sectors. With decreasing snowfall frequencies and the general increase of the snowline (e.g.,  
974 Beniston, 2003; Gobiet et al., 2014; Hantel et al., 2012), both associated with temperature changes,  
975 ski lift operators are looking into an uncertain future. A shorter snowfall season will likely put them  
976 under greater financial pressure. Climate change effects might be manageable only for ski areas  
977 reaching up to high elevations (e.g. Elsasser and Bürki, 2002). Even so these resorts might start later  
978 into the ski season, the snow conditions into early spring could change less dramatically due to  
979 projected high-elevation snowfall increases in mid-winter. A positive aspect of the projected decrease  
980 in snowfall frequency might be a reduced expenditures for airport and road safety (e.g., Zubler et al.,  
981 2015).

982 At lower altitudes, an intensification of winter precipitation, combined with smaller snowfall fractions  
983 (Serquet et al., 2013), increases the flood potential (Beniston, 2012). Snow can act as a buffer by  
984 releasing melt water constantly over a longer period of time. With climate warming, this storage  
985 capacity is lost, and heavy precipitation immediately drains into streams and rivers which might not be  
986 able to take up the vast amount of water fast enough. Less snowmelt will also have impacts on  
987 hydropower generation and water management (e.g., Weingartner et al., 2013). So far, many Alpine  
988 regions are able to bypass dry periods by tapping melt water from mountainous regions. With reduced  
989 snow-packs due to less snowfall, water shortage might become a serious problem in some areas.

990 Regarding specific socio-economic impacts caused by extreme snowfall events, conclusions based on  
991 the results presented in this study are difficult to draw. It might be possible that the 99% all-day  
992 snowfall percentile we used for defining heavy snowfalls, is not appropriate to speculate about future  
993 evolutions of (very) rare events (Schär et al., 2016). To do so, one might consider applying a  
994 generalized extreme value (GEV) analysis which is more suitable for answering questions related to  
995 rare extreme events.

996 **7 Data Availability**

997 The EURO-CORDEX RCM data analysed in the present work are publicly available - parts of  
998 them for non-commercial use only - via the Earth System Grid Federation archive (ESGF;  
999 e.g., <https://esgf-data.dkrz.de>). The observational datasets RHiresD and TabsD as well as  
1000 the snow depth data for Switzerland are available for research and educational purposes  
1001 from [kundendienst@meteoschweiz.ch](mailto:kundendienst@meteoschweiz.ch). The analysis code is available from the  
1002 corresponding author on request.

1003 **8 Competing Interests**

1004 The authors declare that they have no conflict of interest.

1005 **9 Acknowledgements**

1006 We gratefully acknowledge the support of Jan Rajczak, Urs Beyerle and Curdin Spirig (ETH Zurich) as  
1007 well as Elias Zubler (MeteoSwiss) in data acquisition and pre-processing. Christoph Frei (MeteoSwiss)  
1008 and Christoph Marty (WSL-SLF) provided important input on specific aspects of the analysis. The  
1009 GTOPO30 digital elevation model is available from the U.S. Geological Survey. Finally, we thank the  
1010 climate modelling groups of the EURO-CORDEX initiative for producing and making available their  
1011 model output.

1012 **10 References**

- 1013 Abegg, B. A., S., Crick, F., and de Montfalcon, A.: Climate change impacts and adaptation in winter tourism, in:  
1014 Climate change in the European Alps: adapting winter tourism and natural hazards management, edited by:  
1015 Agrawala, S., Organisation for Economic Cooperation and Development (OECD), Paris, France, 25-125, 2007.
- 1016 Allen, M. R., and Ingram, W. J.: Constraints on future changes in climate and the hydrologic cycle, *Nature*, 419,  
1017 224-232, 10.1038/nature01092, 2002.
- 1018 ~~Ban, N., Schmidli, J., and Schär, C.: Heavy precipitation in a changing climate: Does short-term summer~~  
1019 ~~precipitation increase faster?, *Geophys Res Lett*, 42, 1165-1172, 10.1002/2014GL062588, 2015.~~
- 1020 Beniston, M.: Climatic Change in Mountain Regions: A Review of Possible Impacts. *Clim Change*, 59, 5-31.
- 1021 Beniston, M.: Impacts of climatic change on water and associated economic activities in the Swiss Alps, *J Hydrol*,  
1022 412, 291-296, 10.1016/j.jhydrol.2010.06.046, 2012.
- 1023 Ceppi, P., Scherrer, S.C., Fischer, A.M., and Appenzeller, C.: Revisiting Swiss temperature trends 1959–2008, *Int*  
1024 *J Climatol*, 32, 203-213, 10.1002/joc.2260, 2012.
- 1025 CH2011: Swiss Climate Change Scenarios CH2011, published by C2SM, MeteoSwiss, ETH, NCCR Climate, and  
1026 OcCC, Zurich, Switzerland, 88 pp, 2011.
- 1027 Chimani, B., Böhm, R., Matulla, C., and Ganekind, M.: Development of a longterm dataset of solid/liquid  
1028 precipitation, *Adv Sci Res*, 6, 39-43, 10.5194/asr-6-39-2011, 2011.
- 1029 de Vries, H., Haarsma, R. J., Hazeleger, W.: On the future reduction of snowfall in western and central Europe.  
1030 *Clim Dyn*, 41, 2319-2330, 10.1007/s00382-012-1583-x, 2013.
- 1031 de Vries, H., Lenderink, G., and van Meijgaard, E.: Future snowfall in western and central Europe projected with a  
1032 high-resolution regional climate model ensemble, *Geophys Res Lett*, 41, 4294-4299, 10.1002/2014GL059724,  
1033 2014.
- 1034 Deser, C., Knutti, R., Solomon, S. and Phillips, A. S.: Communication of the role of natural variability in future  
1035 North American climate. *Nature Clim Change*, 2, 775-779, 2012.

- 1036 Elsasser, H. and Bürki, R.: Climate change as a threat to tourism in the Alps. *Climate Research*, 20, 253-257.
- 1037 Fischer, A. M., Keller, D. E., Liniger, M. A., Rajczak, J., Schär, C., and Appenzeller, C.: Projected changes in  
1038 precipitation intensity and frequency in Switzerland: a multi-model perspective, *Int J Climatol*, 35, 3204-3219,  
1039 10.1002/joc.4162, 2015.
- 1040 Fischer, E. M. and Knutti, R.: Observed heavy precipitation increase confirms theory and early models. *Nature*  
1041 *Clim Change*, 6, 986-992, 10.1038/NCLIMATE3110, 2016.
- 1042 Frei, C. and Schär, C.: A precipitation climatology of the Alps from high-resolution rain-gauge observations, *Int J*  
1043 *Climatol*, 18, 873-900, 10.1002/(Sici)1097-0088(19980630)18:8<873::Aid-Joc255>3.0.Co;2-9, 1998.
- 1044 Frei, C., Christensen, J. H., Déqué, M., Jacob, D., Jones, R. G., and Vidale, P. L.: Daily precipitation statistics in  
1045 regional climate models: Evaluation and intercomparison for the European Alps, *J Geophys Res-Atmos*, 108,  
1046 10.1029/2002jd002287, 2003.
- 1047 Frei, C.: Interpolation of temperature in a mountainous region using nonlinear profiles and non-Euclidean  
1048 distances, *Int J Climatol*, 34, 1585-1605, 10.1002/joc.3786, 2014.
- 1049 Giorgi, F.: Simulation of regional climate using a limited area model nested in a general circulation model, *J*  
1050 *Climate*, 3, 941-963, 1990.
- 1051 Giorgi, F., Jones, C., and Asrar, G. R.: Addressing climate information needs at the regional level: the CORDEX  
1052 framework, *World Meteorological Organization (WMO) Bulletin*, 58, 175, 2009.
- 1053 Giorgi, F., Torma, C., Coppola, E., Ban, N., Schär, C., and Somot, S.: Enhanced summer convective rainfall at  
1054 Alpine high elevations in response to climate warming, *Nat Geo*, 9, 584-589, 10.1038/ngeo2761, 2016.
- 1055 Gobiet, A., Kotlarski, S., Beniston, M., Heinrich, G., Rajczak, J., and Stoffel, M.: 21st century climate change in  
1056 the European Alps - A review, *Science of the Total Environment*, 493, 1138-1151,  
1057 10.1016/j.scitotenv.2013.07.050, 2014.
- 1058 Grünewald, T., and Lehning, M.: Are flat-field snow depth measurements representative? A comparison of  
1059 selected index sites with areal snow depth measurements at the small catchment scale, *Hydrol Processes*, 29,  
1060 1717-1728, 10.1002/hyp.10295, 2015.
- 1061 Hantel, M., Maurer, C., and Mayer, D.: The snowline climate of the Alps 1961–2010. *Theor Appl Climatol*, 110,  
1062 517, 10.1007/s00704-012-0688-9, 2012.
- 1063 Hawkins, E., and Sutton, R.: The Potential to Narrow Uncertainty in Regional Climate Predictions, *B Am Meteorol*  
1064 *Soc*, 90, 1095+, 10.1175/2009BAMS2607.1, 2009.
- 1065 Haylock, M.R., Hofstra, N., Klein Tank, A.M.G., Klok, E.J., Jones, P.D., and New, M.: A European daily high-  
1066 resolution gridded data set of surface temperature and precipitation for 1950–2006, *J Geophys Res*, 113,  
1067 D20119, 10.1029/2008JD010201.
- 1068 Held, I. M., and Soden, B. J.: Robust responses of the hydrological cycle to global warming, *J Climate*, 19, 5686-  
1069 5699, 10.1175/Jcli3990.1, 2006.
- 1070 IPCC: *Climate Change 2013: The Physical Science Basis. Contribution of Working Group I to the Fifth*  
1071 *Assessment Report of the Intergovernmental Panel on Climate Change*, Cambridge University Press, Cambridge,  
1072 United Kingdom and New York, NY, USA, 1535 pp., 2013.
- 1073 Isotta, F. A., Frei, C., Weiguni, V., Tadic, M. P., Lassegues, P., Rudolf, B., Pavan, V., Cacciamani, C., Antolini,  
1074 G., Ratto, S. M., Munari, M., Micheletti, S., Bonati, V., Lussana, C., Ronchi, C., Panettieri, E., Marigo, G., and  
1075 Vertacnik, G.: The climate of daily precipitation in the Alps: development and analysis of a high-resolution grid  
1076 dataset from pan-Alpine rain-gauge data, *Int J Climatol*, 34, 1657-1675, 10.1002/joc.3794, 2014.
- 1077 Jacob, D., Petersen, J., Eggert, B., Alias, A., Christensen, O. B., Bouwer, L. M., Braun, A., Colette, A., Déqué, M.,  
1078 Georgievski, G., Georgopoulou, E., Gobiet, A., Menut, L., Nikulin, G., Haensler, A., Hempelmann, N., Jones, C.,  
1079 Keuler, K., Kovats, S., Kröner, N., Kotlarski, S., Kriegsman, A., Martin, E., van Meijgaard, E., Moseley, C.,  
1080 Pfeifer, S., Preuschmann, S., Radermacher, C., Radtke, K., Rechid, D., Rounsevell, M., Samuelsson, P., Somot,  
1081 S., Soussana, J. F., Teichmann, C., Valentini, R., Vautard, R., Weber, B., and Yiou, P.: EURO-CORDEX: new  
1082 high-resolution climate change projections for European impact research, *Reg Environ Change*, 14, 563-578,  
1083 10.1007/s10113-013-0499-2, 2014.
- 1084 Keller, D. E., Fischer, A. M., Liniger, M. A., Appenzeller, C. and Knutti, R.: Testing a weather generator for  
1085 downscaling climate change projections over Switzerland. *Int J Climatol*, doi:10.1002/joc.4750, 2016.
- 1086 Kienzle, S. W.: A new temperature based method to separate rain and snow, *Hydrol Process*, 22, 5067-5085,  
1087 10.1002/hyp.7131, 2008.
- 1088 Kotlarski, S., Bosshard, T., Lüthi, D., Pall, P., and Schär, C.: Elevation gradients of European climate change in  
1089 the regional climate model COSMO-CLM. *Clim Change*, 112, 189-215, 10.1007/s10584-011-0195-5, 2012.
- 1090 Kotlarski, S., Keuler, K., Christensen, O. B., Colette, A., Deque, M., Gobiet, A., Goergen, K., Jacob, D., Luthi, D.,  
1091 van Meijgaard, E., Nikulin, G., Schar, C., Teichmann, C., Vautard, R., Warrach-Sagi, K., and Wulfmeyer, V.:

- 1092 Regional climate modeling on European scales: a joint standard evaluation of the EURO-CORDEX RCM  
1093 ensemble, *Geosci Model Dev*, 7, 1297-1333, 10.5194/gmd-7-1297-2014, 2014.
- 1094 Kotlarski, S., Lüthi, D., and Schär, C.: The elevation dependency of 21st century European climate change: an  
1095 RCM ensemble perspective, *Int J Climatol*, 35, 3902-3920, 10.1002/joc.4254, 2015.
- 1096 Krasting, J. P., Broccoli, A. J., Dixon, K. W., and Lanzante, J. R.: Future Changes in Northern Hemisphere  
1097 Snowfall. *J Clim*, 26, 7813-7828, 10.1175/JCLI-D-12-00832.1, 2013.
- 1098 Laternser, M., and Schneebeli, M.: Long-term snow climate trends of the Swiss Alps (1931-99), *Int J Climatol*, 23,  
1099 733-750, 10.1002/joc.912, 2003.
- 1100 Marty, C.: Regime shift of snow days in Switzerland, *Geophys Res Lett*, 35, 10.1029/2008gl033998, 2008.
- 1101 Marty, C., and Blanchet, J.: Long-term changes in annual maximum snow depth and snowfall in Switzerland  
1102 based on extreme value statistics, *Climatic Change*, 111, 705-721, 2011.
- 1103 McAfee, S. A., Walsh, J., and Rupp, T. S.: Statistically downscaled projections of snow/rain partitioning for  
1104 Alaska, *Hydrol Process*, 28, 3930-3946, 10.1002/hyp.9934, 2014.
- 1105 MeteoSchweiz: Klimareport 2015. Bundesamt für Meteorologie und Klimatologie MeteoSchweiz, Zürich.
- 1106 MeteoSwiss: Daily Precipitation (final analysis): RhiresD:  
1107 www.meteoswiss.admin.ch/content/dam/meteoswiss/de/service-und-publikationen/produkt/raeumliche-daten-  
1108 niederschlag/doc/ProdDoc\_RhiresD.pdf, access: 10.01.2017, 2013a.
- 1109 MeteoSwiss: Daily Mean, Minimum and Maximum Temperature: TabsD, TminD ,TmaxD:  
1110 www.meteoswiss.admin.ch/content/dam/meteoswiss/de/service-und-publikationen/produkt/raeumliche-daten-  
1111 temperatur/doc/ProdDoc\_TabsD.pdf, access: 10.01.2017, 2013b.
- 1112 Moss, R. H., Edmonds, J. A., Hibbard, K. A., Manning, M. R., Rose, S. K., van Vuuren, D. P., Carter, T. R., Emori,  
1113 S., Kainuma, M., Kram, T., Meehl, G. A., Mitchell, J. F. B., Nakicenovic, N., Riahi, K., Smith, S. J., Stouffer, R. J.,  
1114 Thomson, A. M., Weyant, J. P., and Wilbanks, T. J.: The next generation of scenarios for climate change research  
1115 and assessment, *Nature*, 463, 747-756, 10.1038/nature08823, 2010.
- 1116 Neff, E. L.: How Much Rain Does a Rain Gauge Gauge, *J Hydrol*, 35, 213-220, 10.1016/0022-1694(77)90001-4,  
1117 1977.
- 1118 O'Gorman, P. A.: Contrasting responses of mean and extreme snowfall to climate change, *Nature*, 512, 416-  
1119 U401, 10.1038/nature13625, 2014.
- 1120 Piazza, M., Boé, J., Terray, L., Pagé, C., Sanchez-Gomez, E., and Déqué, M.: Projected 21st century snowfall  
1121 changes over the French Alps and related uncertainties, *Climatic Change*, 122, 583-594, 10.1007/s10584-013-  
1122 1017-8, 2014.
- 1123 Räisänen, J.: Twenty-first century changes in snowfall climate in Northern Europe in ENSEMBLES regional  
1124 climate models, *Clim Dynam*, 46, 339-353, 10.1007/s00382-015-2587-0, 2016.
- 1125 Rajczak, J., Pall, P., and Schär, C.: Projections of extreme precipitation events in regional climate simulations for  
1126 Europe and the Alpine Region, *J Geophys Res-Atmos*, 118, 3610-3626, 10.1002/jgrd.50297, 2013.
- 1127 Rajczak, J., Kotlarski, S., and Schär, C.: Does Quantile Mapping of Simulated Precipitation Correct for Biases in  
1128 Transition Probabilities and Spell Lengths?, *J Climate*, 29, 1605-1615, 10.1175/Jcli-D-15-0162.1, 2016.
- 1129 ~~Rajczak, J. and Schär, C.: Projections of future precipitation extremes over Europe: A multi-model assessment of  
1130 climate simulations. In preparation.~~ Rajczak, J. and Schär, C.: Projections of future precipitation extremes over  
1131 Europe: a multi-model assessment of climate simulations. *J Geophys Res Atmos*, in press, 2017.
- 1132 Richards, F. J.: A Flexible Growth Function for Empirical Use, *J Exp Bot*, 10, 290-300, 10.1093/Jxb/10.2.290,  
1133 1959.
- 1134 Rummukainen, M.: State-of-the-art with regional climate models, *Wiley Interdisciplinary Reviews-Climate Change*,  
1135 1, 82-96, 10.1002/wcc.8, 2010.
- 1136 Schär, C., Ban, N., Fischer, E. M., Rajczak, J., Schmidli, J., Frei, C., Giorgi, F., Karl, T. R., Kendon, E. J., Tank, A.  
1137 M. G. K., O'Gorman, P. A., Sillmann, J., Zhang, X. B., and Zwiers, F. W.: Percentile indices for assessing changes  
1138 in heavy precipitation events, *Climatic Change*, 137, 201-216, 10.1007/s10584-016-1669-2, 2016.
- 1139 Scherrer, S. C., Appenzeller, C., and Laternser, M.: Trends in Swiss Alpine snow days: The role of local- and  
1140 large-scale climate variability, *Geophys Res Lett*, 31, 10.1029/2004gl020255, 2004.
- 1141 Schmidli, J., Frei, C., and Vidale, P. L.: Downscaling from GCM precipitation: A benchmark for dynamical and  
1142 statistical downscaling methods, *Int J Climatol*, 26, 679-689, 10.1002/joc.1287, 2006.
- 1143 Schmucki, E., Marty, C., Fierz, C., and Lehning, M.: Simulations of 21st century snow response to climate change  
1144 in Switzerland from a set of RCMs, *Int J Climatol*, 35, 3262-3273, 10.1002/joc.4205, 2015a.
- 1145 Schmucki, E., Marty, C., Fierz, C., Weingartner, R. and Lehning, M.: Impact of climate change in Switzerland on  
1146 socioeconomic snow indices, *Theor Appl Climatol*, in press, 10.1007/s00704-015-1676-7, 2015b.

1147 Serquet, G., Marty, C., and Rebetez, M.: Monthly trends and the corresponding altitudinal shift in the  
1148 snowfall/precipitation day ratio, *Theor Appl Climatol*, 114, 437-444, 10.1007/s00704-013-0847-7, 2013.  
1149 Sevruck, B.: Der Niederschlag in der Schweiz, Geographisches Institut der Eidgenössischen Technischen Hochschule in  
1150 Zürich, Abteilung Hydrologie, Zurich, Switzerland, 1985.

1151 SFOE, Hydropower: <http://www.bfe.admin.ch/themen/00490/00491/index.html?lang=en>, access: 16.09.2016,  
1152 2014.

1153 Smiatek, G., Kunstmann, H., and Senatore, A.: EURO-CORDEX regional climate model analysis for the Greater  
1154 Alpine Region: Performance and expected future change, *J Geophys Res-Atmos*, 121, 7710-7728,  
1155 10.1002/2015JD024727, 2016.

1156 Soncini, A., and Bocchiola, D.: Assessment of future snowfall regimes within the Italian Alps using general  
1157 circulation models, *Cold Reg Sci Technol*, 68, 113-123, 10.1016/j.coldregions.2011.06.011, 2011.

1158 Steger, C., Kotlarski, S., Jonas, T., and Schär, C.: Alpine snow cover in a changing climate: a regional climate  
1159 model perspective, *Clim Dynam*, 41, 735-754, 10.1007/s00382-012-1545-3, 2013.

1160 Techel, F., Stucki, T., Margreth, S., Marty, C., and Winkler, K.: Schnee und Lawinen in den Schweizer Alpen.  
1161 Hydrologisches Jahr 2013/14, WSL-Institut für Schnee- und Lawinenforschung SLF, Birmensdorf, Switzerland,  
1162 2015.

1163 Terzago, S., von Hardenberg, J., Palazzi, E., and Provenzale, A.: Snow water equivalent in the Alps as seen by  
1164 gridded datasets, CMIP5 and CORDEX climate models. *The Cryosphere Discussion*, 10.5194/tc-2016-280, 2017.

1165 Torma, C., Giorgi, F., and Coppola, E.: Added value of regional climate modeling over areas characterized by  
1166 complex terrain Precipitation over the Alps, *J Geophys Res-Atmos*, 120, 3957-3972, 10.1002/2014JD022781,  
1167 2015.

1168 Vautard, R., Gobiet, A., Jacob, D., Belda, M., Colette, A., Déqué, M., Fernandez, J., Garcia-Diez, M., Goergen,  
1169 K., Guttler, I., Halenka, T., Karacostas, T., Katragkou, E., Keuler, K., Kotlarski, S., Mayer, S., van Meijgaard, E.,  
1170 Nikulin, G., Patarcic, M., Scinocca, J., Sobolowski, S., Suklitsch, M., Teichmann, C., Warrach-Sagi, K.,  
1171 Wulfmeyer, V., and Yiou, P.: The simulation of European heat waves from an ensemble of regional climate  
1172 models within the EURO-CORDEX project, *Clim Dynam*, 41, 2555-2575, 10.1007/s00382-013-1714-z, 2013.

1173 Weingartner, R., Schädler, B., and Hänggi, P.: Auswirkungen der Klimaänderung auf die schweizerische  
1174 Wasserkraftnutzung, *Geographica Helvetica*, 68, 239-248, 2013.

1175 Yang, D. Q., Elomaa, E., Tuominen, A., Aaltonen, A., Goodison, B., Gunther, T., Golubev, V., Sevruck, B.,  
1176 Madsen, H., and Milkovic, J.: Wind-induced precipitation undercatch of the Hellmann gauges, *Nord Hydrol*, 30,  
1177 57-80, 1999.

1178 Zubler, E. M., Scherrer, S. C., Croci-Maspoli, M., Liniger, M. A., and Appenzeller, C.: Key climate indices in  
1179 Switzerland; expected changes in a future climate, *Climate Change*, 123, 255-271, 10.1007/s10584-013-1041-8,  
1180 2014.

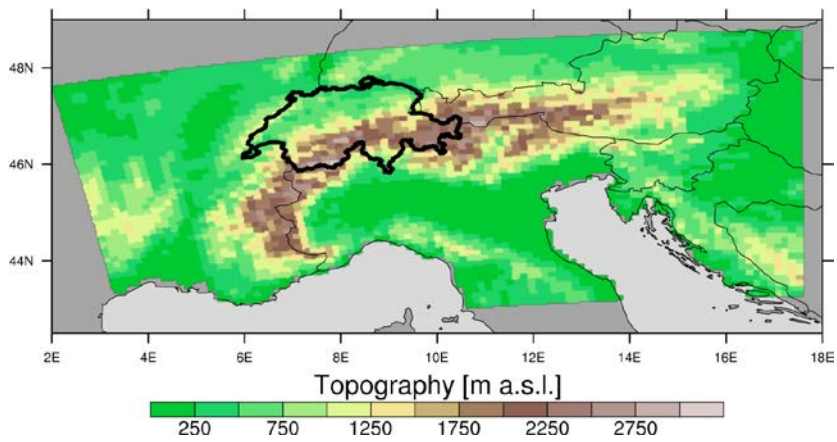
1181 Zubler, E. M., Fischer, A. M., Liniger, M. A., and Schlegel, T.: Auftausalzverbrauch im Klimawandel, *MeteoSwiss*,  
1182 Zürich, Switzerland, Fachbericht 253, 2015.

1183

1184 **Figures**

1185

1186

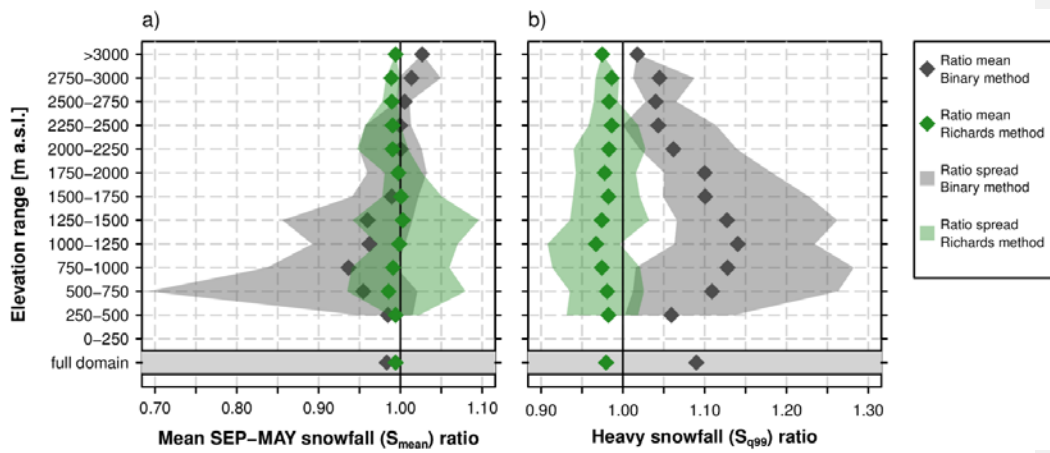


1187

1188

1189 **Figure 1** GTOPO30 topography (<https://ta.cr.usgs.gov/GTOPO30>) aggregated to the EUR-11 (0.11°) RCM grid.  
1190 The coloured area shows the Alpine domain used for the assessment of snowfall projections. The bold black  
1191 outline marks the Swiss sub-domain used for the assessment of the bias adjustment approach.

1192



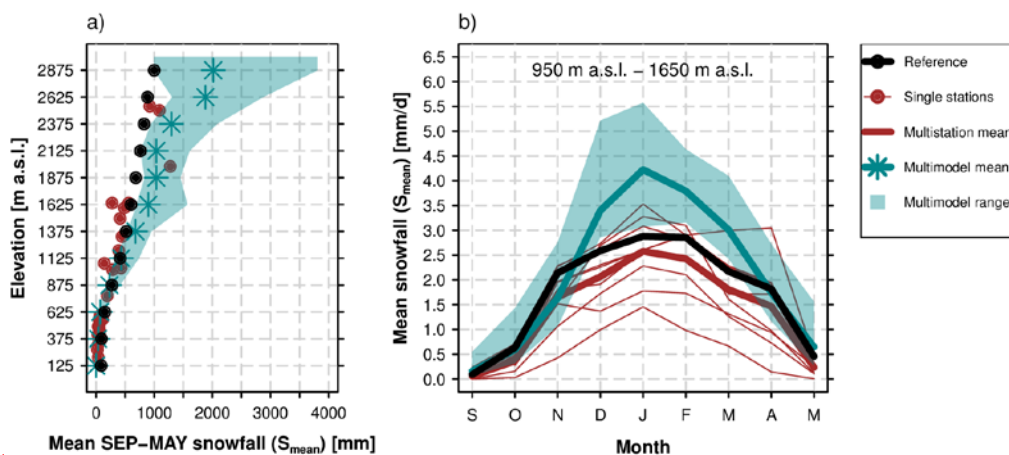
1193  
1194

1195 **Figure 2** Snowfall ratios for the Binary and Richards snow fractionation method. Ratios represent the quotient  
 1196 (ratio between of the snowfall as estimated by of the respective method and the snowfall as estimated by the  
 1197 Subgrid method). The ratios are valid at the coarse-resolution grid (12 km). a) Ratios for mean snowfall,  $S_{mean}$ .  
 1198 b) Ratios for heavy snowfall,  $S_{q99}$ . Ratio means were derived after averaging the corresponding snowfall index for  
 1199 250 m elevation intervals in Switzerland while the ratio spread represents the minimum and maximum grid point-  
 1200 based ratios in the corresponding elevation interval. This analysis is entirely based on the observational data sets  
 1201 TabsD and RhiresD.

1202



1203

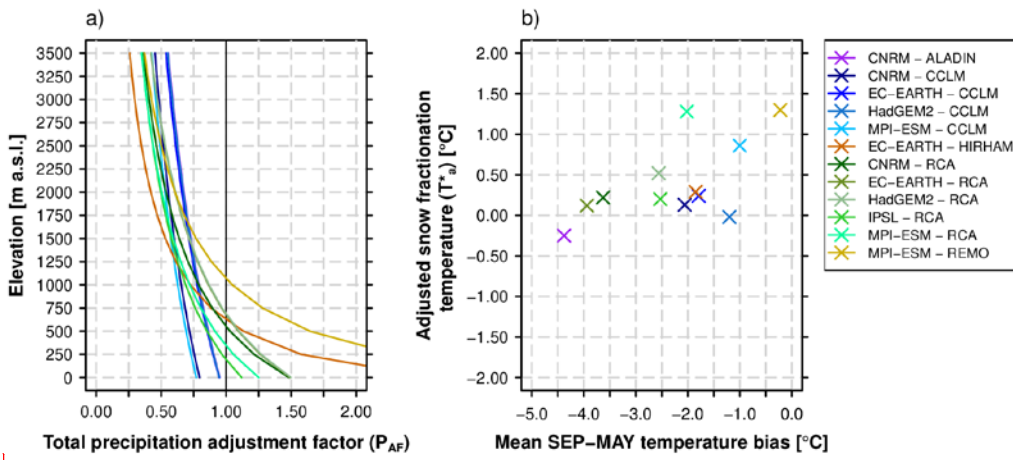


1204

1205 **Figure 3** Comparison of measured fresh snow sums of 29 MeteoSwiss stations (red) against simulated RCM raw  
1206 snowfall in Switzerland (green) and against the 2 km reference snowfall grid obtained by employing the *Subgrid*  
1207 *method* (black) in the EVAL period 1971-2005. a) Mean September – May snowfall vs. elevation. Both the  
1208 simulation data (green) and the reference data (black) are based on the spatio-temporal mean of 250 m elevation  
1209 ranges and plotted at the mean elevation of the corresponding interval. b) Seasonal September-May snowfall  
1210 cycle for the elevation interval 950 m a.s.l. to 1650 m a.s.l.. Simulated multi-model means and spreads are based  
1211 on a subset of [seven9](#) EURO-CORDEX simulations providing raw snowfall as output variable (see Tab. 1).

1212

**Comment [Sven1]:** Figure revised due to removal of two further model chains.



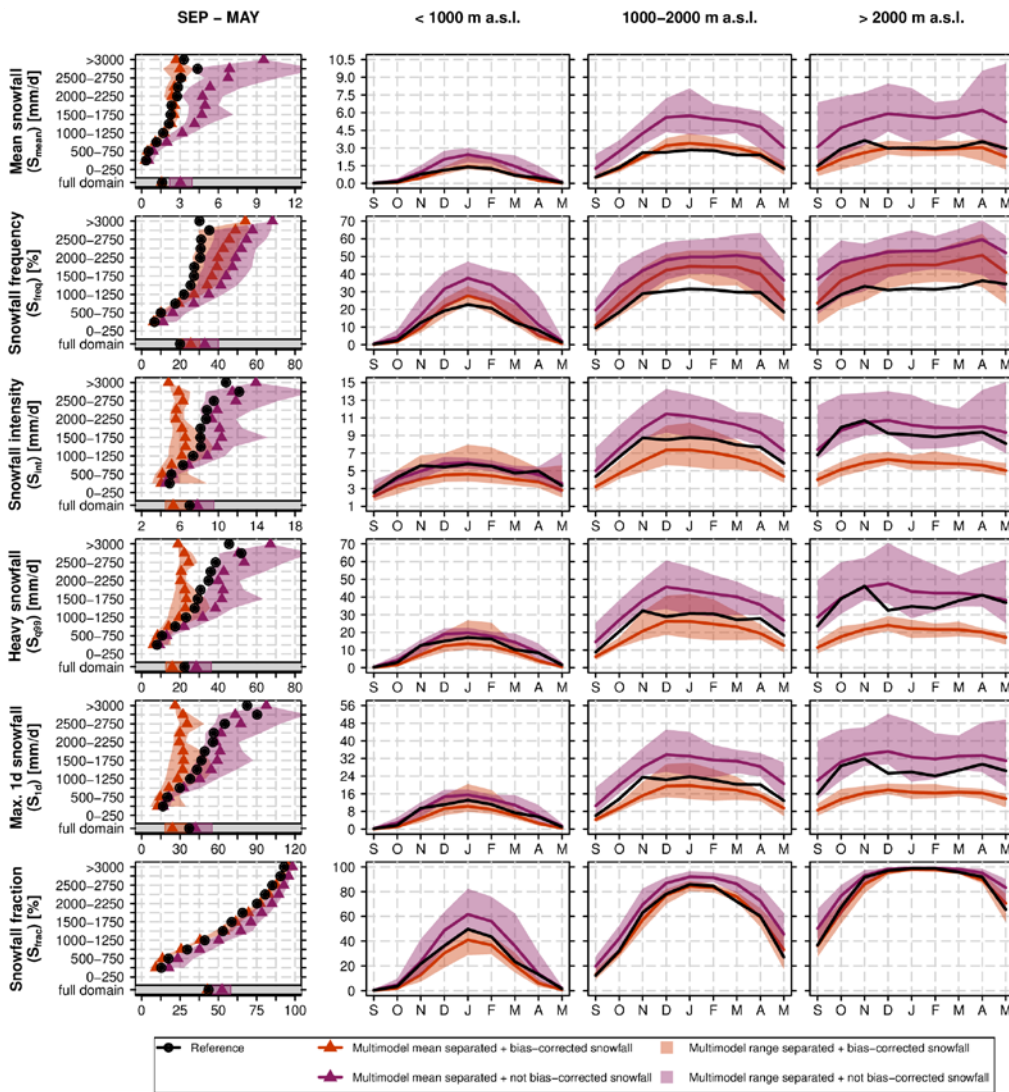
1213

1214  
1215  
1216

**Figure 4** Overview of bias adjustment. a) Elevation-dependent total precipitation adjustment factors,  $P_{AF}$ , for the 124 GCM-RCM chains (see Eq. 10). b) Scatterplot of mean September to May temperature biases (RCM simulation minus observational analysis) vs. adjusted snow fractionation temperatures,  $T^*_a$ .

Comment [Sven2]: Figure revised due to removal of two further model chains.

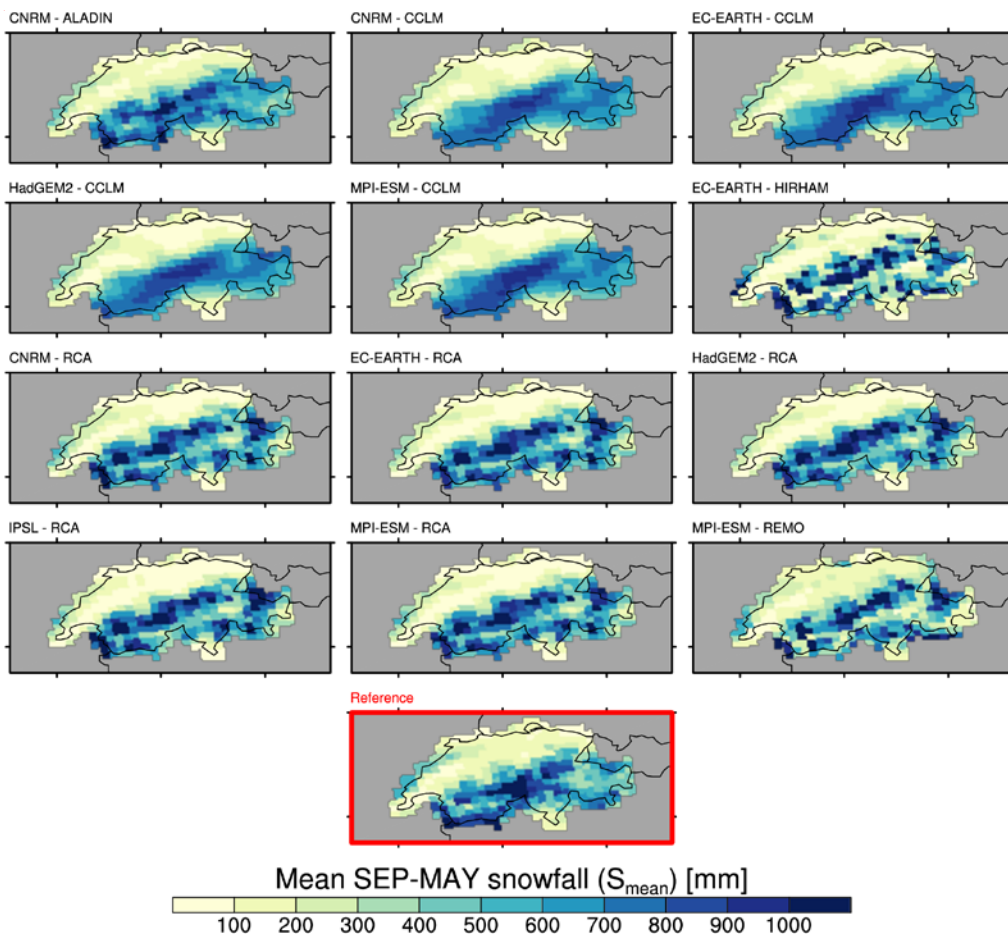
Comment [Sven3]: Figure revised due to removal of two further model chains.



1217  
1218

1219 **Figure 5** Evaluation of snowfall indices in the EVAL period 1971-2005 for the 124 snowfall separated + bias-  
 1220 adjusted (RCM<sub>sep+ba</sub>) and 124 snowfall separated + not bias-adjusted (RCM<sub>sep+nba</sub>) RCM simulations vs.  
 1221 observation-based reference. The first column shows the mean September-May snowfall index statistics vs.  
 1222 elevation while the monthly snowfall indices (spatially averaged over the elevation intervals <1000 m.a.s.l., 1000  
 1223 m a.s.l.-2000 m a.s.l. and >2000 m a.s.l.) are displayed in columns 2-4.

1224



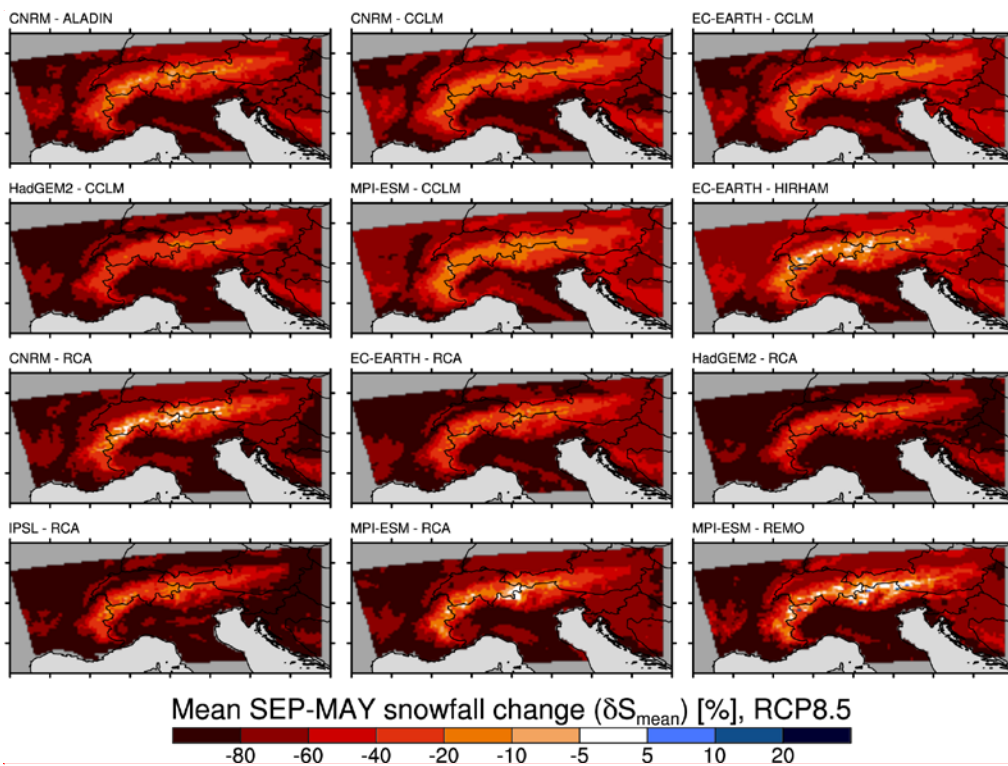
Comment [Sven4]: Figure revised due to removal of two further model chains.

1225  
1226

1227  
1228  
1229

**Figure 6** Spatial distribution of mean September-May snowfall,  $S_{\text{mean}}$ , in the EVAL period 1971-2005 and for the 124 snowfall separated + bias-adjusted RCM simulations ( $\text{RCM}_{\text{sep+ba}}$ ). In the lower right panel, the map of the Bottom panel: observation-based reference is shown.

1230

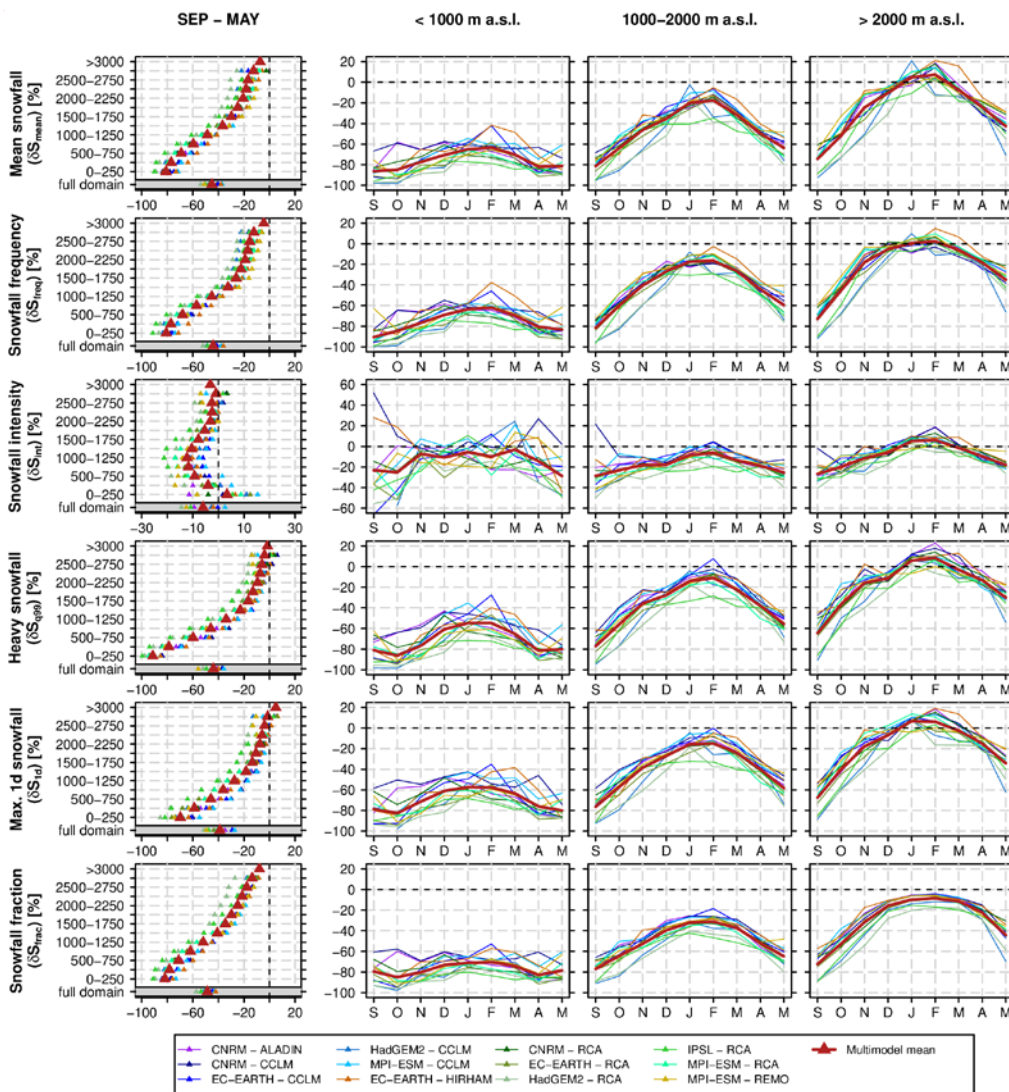


Comment [Sven5]: Figure revised due to removal of two further model chains.

1231  
1232

1233 **Figure 7** Spatial distribution of relative changes (SCEN period 2070-2099 with respect to CTRL period 1981-  
1234 2010) in mean September-May snowfall,  $\delta S_{\text{mean}}$ , for RCP8.5 and for the 124 snowfall separated + bias-adjusted  
1235 RCM simulations ( $\text{RCM}_{\text{sep+ba}}$ ). For RCP4.5, see Fig. S6.

1236



Comment [Sven6]: Figure revised due to removal of two further model chains.

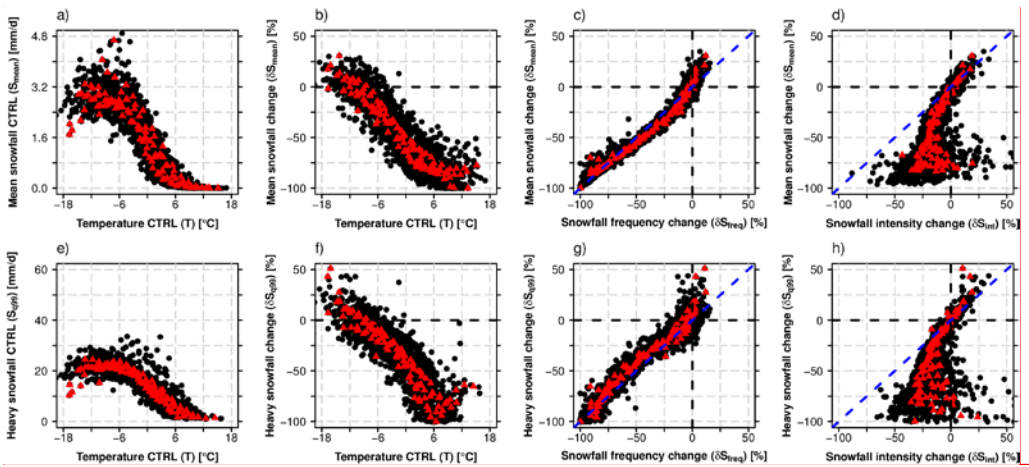
1237  
1238

1239  
1240  
1241  
1242  
1243

**Figure 8** Relative changes (SCEN period 2070-2099 with respect to CTRL period 1981-2010) of snowfall indices based on the 124 snowfall separated + bias-adjusted RCM simulations (RCM<sub>sep+ba</sub>) for RCP8.5. The first column shows the mean September-May snowfall index statistics vs. elevation while monthly snowfall index changes (spatially averaged over the elevation intervals <1000 m.a.s.l., 1000 m a.s.l.-2000 m a.s.l. and >2000 m a.s.l.) are displayed in columns 2-4.

1244





Comment [Sven7]: Figure revised due to removal of two further model chains.

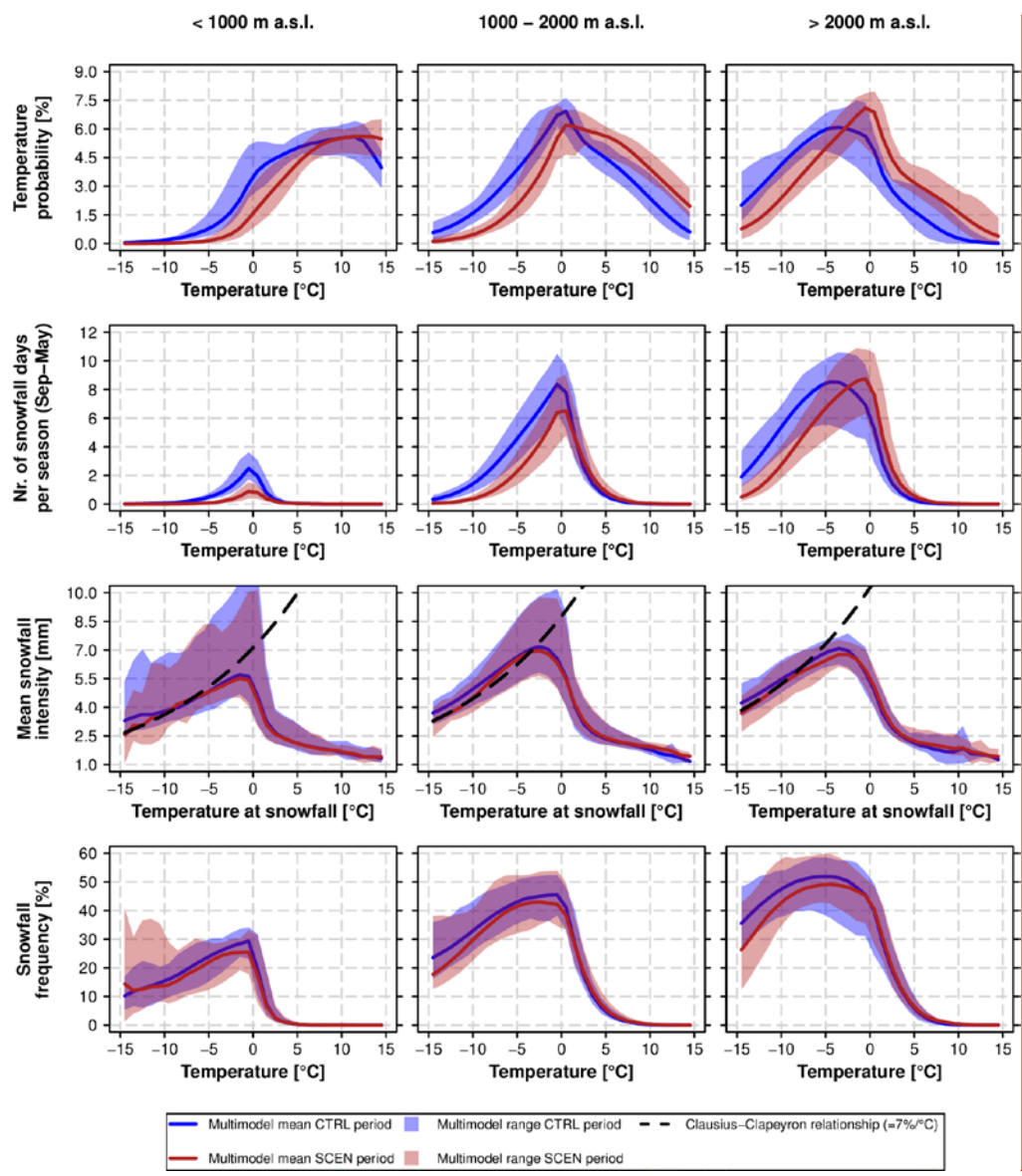
1245  
1246

1247  
1248  
1249  
1250  
1251  
1252  
1253

**Figure 9** Intercomparison of various snowfall indices and relationship with monthly mean temperature in CTRL. For each panel, the monthly mean statistics for each 250 m elevation interval and for each of the 124 individual GCM-RCM chains were derived (black circles). Red triangles denote the multi-model mean for a specific month and elevation interval. The monthly statistics were calculated by considering all grid points of the specific elevation intervals which are available for both variables in the corresponding scatterplot only (area consistency). The data were taken from the 124 snowfall separated + bias-adjusted (RCM<sub>sep+ba</sub>) RCM simulations. Relative changes are based on the RCP8.5 driven simulations (SCEN 2070-2099 wrt. CTRL 1981-2010).

1254

Comment [Sven8]: Figure revised due to removal of two further model chains.

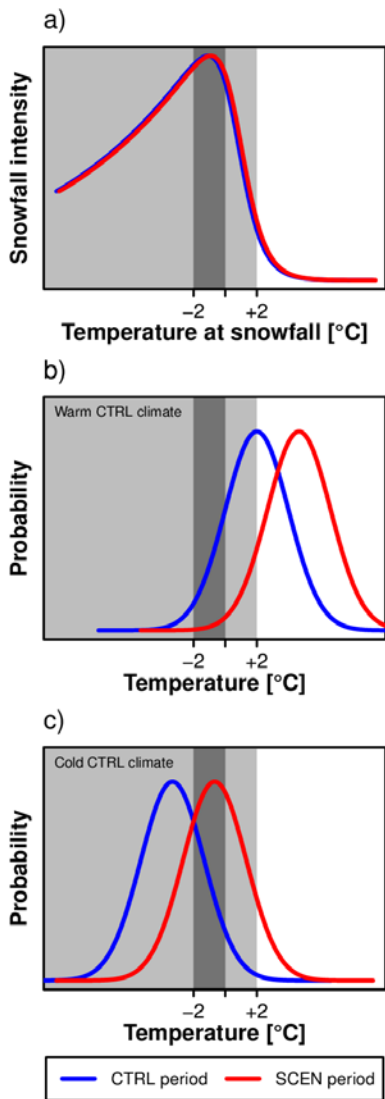


1255

1256

1257 **Figure 10** Comparison of temperature probability, snowfall probability and mean snowfall intensity for the CTRL  
 1258 period 1981-2010 and SCEN period 2070-2099 for RCP8.5. The analysis is based on data from the 124 snowfall  
 1259 separated + bias-adjusted RCM simulations (RCM<sub>sep+ba</sub>). The top row depicts the PDF of the daily temperature  
 1260 distribution, while the second row shows the mean number of snowfall days between September and May, i.e.,  
 1261 days with  $S > 1$  mm (see Tab. 2), in a particular temperature interval. The third row represents the mean snowfall  
 1262 intensity,  $S_{int}$ , for a given snowfall temperature interval. In addition the Clausius-Clapeyron relationship, centred at  
 1263 the  $-10^{\circ}\text{C}$  mean  $S_{int}$  for SCEN, is displayed by the black dashed line. PDFs and mean  $S_{int}$  were calculated by  
 1264 creating daily mean temperature bins of width  $1^{\circ}\text{C}$ .

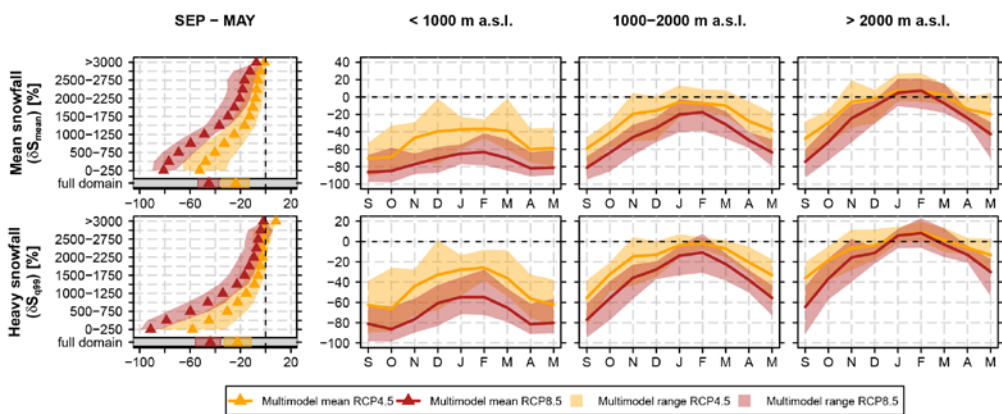




1265  
1266

1267 **Figure 11** Schematic illustration of the control of changes in snowfall intensity on changes in mean and extreme  
 1268 snowfall. a) Relation between temperature and mean snowfall intensity. b) Daily temperature PDF for a warm  
 1269 control climate (low elevations or transition seasons, i.e., beginning or end of winter). c) Daily temperature PDF  
 1270 for a cold control climate (high elevations or mid-winter). The blue line denotes the historical CTRL period, the red  
 1271 line the future SCEN period. The light grey shaded area represents the overall temperature interval at which  
 1272 snowfall occurs, the dark grey shading shows the preferred temperature interval for heavy snowfall to occur.

1273



Comment [Sven9]: Figure revised due to removal of two further model chains.

1274

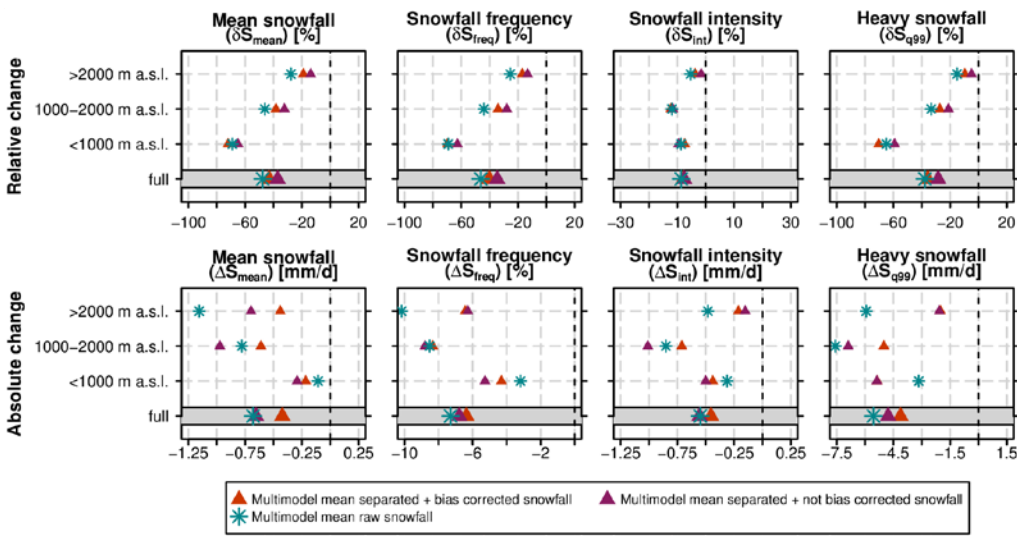
1275

1276

1277

**Figure 12** Similar as Figure 8 but showing projected changes of mean snowfall,  $\delta S_{\text{mean}}$ , and heavy snowfall,  $\delta S_{99}$ , for the emission scenarios RCP4.5 and 8.5. See Fig. S109 for the emission scenario uncertainty of the remaining four snowfall indices.

1278



Comment [Sven10]: Figure revised due to removal of two further model chains.

1279  
1280

1281 **Figure 13** Relative and absolute changes (SCEN period 2070-2099 with respect to CTRL period 1981-2010) of  
 1282 mean September-May snowfall indices based on a subset of **seven** snowfall separated + bias-adjusted  
 1283 ( $RCM_{sep+ba}$ ), **seven** snowfall separated + not bias-adjusted ( $RCM_{sep+nba}$ ) and **seven** raw snowfall RCM  
 1284 simulations ( $RCM_{raw}$ ) for RCP8.5. Only RCM simulations providing raw snowfall as output variable (see Tab. 1)  
 1285 were used in this analysis.

1286

1287 **Tables**

1288

1289 **Table 1** Overview on the 124 EURO-CORDEX simulations available for this study. The whole model set consists  
 1290 of ~~five~~ seven RCMs driven by five different GCMs. All experiments were realized on a grid, covering the European  
 1291 domain, with a horizontal resolution of approximately 12 km (EUR-11) and were run for the emission scenarios  
 1292 ~~control~~-RCP4.5 and RCP8.5 ~~scenarios within the considered time periods of interest~~. A subset of ~~seven~~ 9  
 1293 simulations provides raw snowfall, i.e., snowfall flux in kg/m<sup>2</sup>s, as output variable. For full institutional names the  
 1294 reader is referred to the official EURO-CORDEX website [www.euro-cordex.net](http://www.euro-cordex.net). Note that the EC-EARTH-driven  
 1295 experiments partly employ different realizations of the GCM run, i.e., explicitly sample the influence of internal  
 1296 climate variability in addition to model uncertainty.

RCM	GCM	Acronym	Institute ID	Raw snowfall output
ALADIN53	CNRM-CERFACS-CNRM-CM5	CNRM - ALADIN	CNRM	no
CCLM4-8-17	CNRM-CERFACS-CNRM-CM5	CNRM - CCLM	CLMcom/BTU	no
CCLM4-8-17	ICHEC-EC-EARTH <del>***</del>	EC-EARTH - CCLM	CLMcom/BTU	no
CCLM4-8-17	MOHC-HadGEM2-ES	HadGEM2 - CCLM	CLMcom/ETH	no
CCLM4-8-17	MPI-M-MPI-ESM-LR	MPI-ESM - CCLM	CLMcom/BTU	no
HIRHAM5	ICHEC-EC-EARTH <del>**</del>	EC-EARTH - HIRHAM	DMI	yes
<del>RACMO22E</del>	<del>ICHEC-EC-EARTH</del>	<del>EC-EARTH - RACMO</del>	<del>KNMI</del>	<del>yes</del>
RCA4	CNRM-CERFACS-CNRM-CM5	CNRM - RCA	SMHI	yes
RCA4	ICHEC-EC-EARTH <del>***</del>	EC-EARTH - RCA	SMHI	yes
RCA4	MOHC-HadGEM2-ES	HadGEM2 - RCA	SMHI	yes
RCA4	IPSL-IPSL-CM5A-MR	IPSL - RCA	SMHI	yes
RCA4	MPI-M-MPI-ESM-LR	MPI-ESM - RCA	SMHI	yes
REMO2009	MPI-M-MPI-ESM-LR <del>*</del>	MPI-ESM - REMO <del>*</del>	MPI-CSC	yes
<del>WRF331F</del>	<del>IPSL-IPSL-CM5A-MR</del>	<del>IPSL - WRF</del>	<del>IPSL-INNERIS</del>	<del>yes</del>

\* r1i1p1 realisation  
 \*\* ~~r3i1p1~~ realisation  
 \*\*\* ~~r12i1p1~~ realisation

1297

1298

1299 **Table 2** Analysed snowfall indices. The last column indicates the threshold value in the CTRL period for  
 1300 considering a grid cell in the climate changes analysis (grid cells with smaller values are skipped for the  
 1301 respective analysis); first number: threshold for monthly analyses, second number: threshold for seasonal  
 1302 analysis.

Index name	Acronym	Unit	Definition	Threshold for monthly / seasonal analysis
Mean snowfall	$S_{\text{mean}}$	mm	(Spatio-)temporal mean snowfall in mm snow water equivalent (only "mm" thereafter).	1 mm / 10 mm
Heavy snowfall	$S_{\text{q99}}$	mm/d	Grid point-based 99% all day snowfall percentile.	1 mm / 1 mm
Max. 1 day snowfall	$S_{\text{1d}}$	mm/d	Mean of each season's or month's maximum 1 day snowfall.	1 mm / 1 mm
Snowfall frequency	$S_{\text{freq}}$	%	Percentage of days with snowfall $S > 1\text{mm/d}$ within a specific time period.	1 % / 1 %
Snowfall intensity	$S_{\text{int}}$	mm/d	Mean snowfall intensity at days with snowfall $S > 1\text{mm/d}$ within a specific time period.	$S_{\text{freq}}$ threshold passed
Snowfall fraction	$S_{\text{frac}}$	%	Percentage of total snowfall, $S_{\text{tot}}$ , on total precipitation, $P_{\text{tot}}$ , within a specific time period.	1 % / 1 %

1303  
 1304  
 1305

1306 **Future snowfall in the Alps: Projections based on the**  
1307 **EURO-CORDEX regional climate models**

1308 Prisco Frei<sup>1</sup>, Sven Kotlarski<sup>2,\*</sup>, Mark A. Liniger<sup>2</sup>, Christoph Schär<sup>1</sup>  
1309

1310 <sup>1</sup>Institute for Atmospheric and Climate Sciences, ETH Zurich, CH-8006, Zurich, Switzerland

1311 <sup>2</sup>Federal Office of Meteorology and Climatology, MeteoSwiss, CH-8058 Zurich-Airport,  
1312 Switzerland

1313  
1314 \* Corresponding author: [sven.kotlarski@meteoswiss.ch](mailto:sven.kotlarski@meteoswiss.ch)

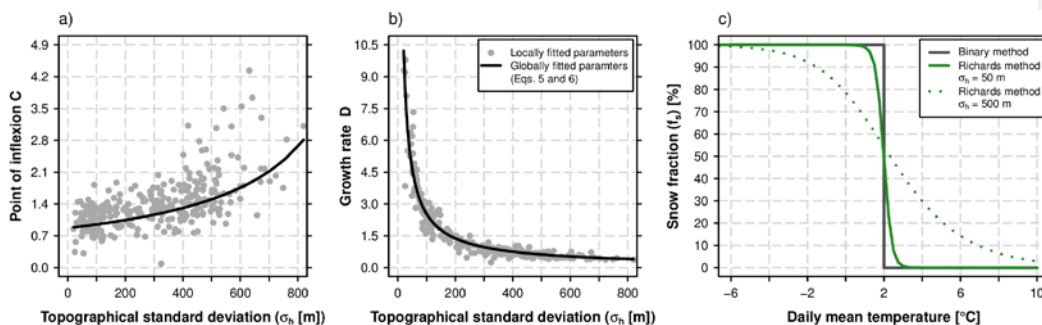
1315

1316 **- Supplementary Material -**

1317

1318

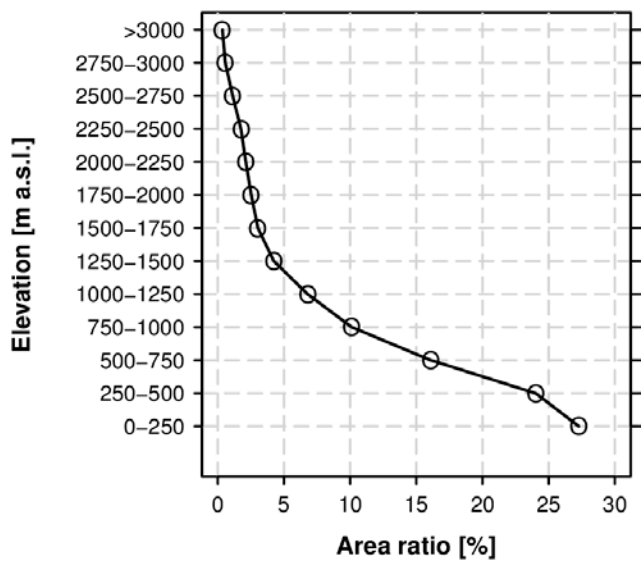
1319



1320

1321 **Figure S1** a) and b) Expressing the point of inflexion C and the growth rate D of the Richards equation as a  
1322 function of the subgrid topographical standard deviation. Grey circles: Fitted parameters for each grid cell in the  
1323 Swiss domain. Black line: Global fit. c) Example for deriving the daily snow fraction  $sf$  based on the binary method  
1324 with a snow fractionation temperature  $T = 2^\circ\text{C}$  (gray line) and based on the Richards method assuming subgrid  
1325 topographical standard deviations of 50 m (solid green line) and 500 m (dotted green line).

1326

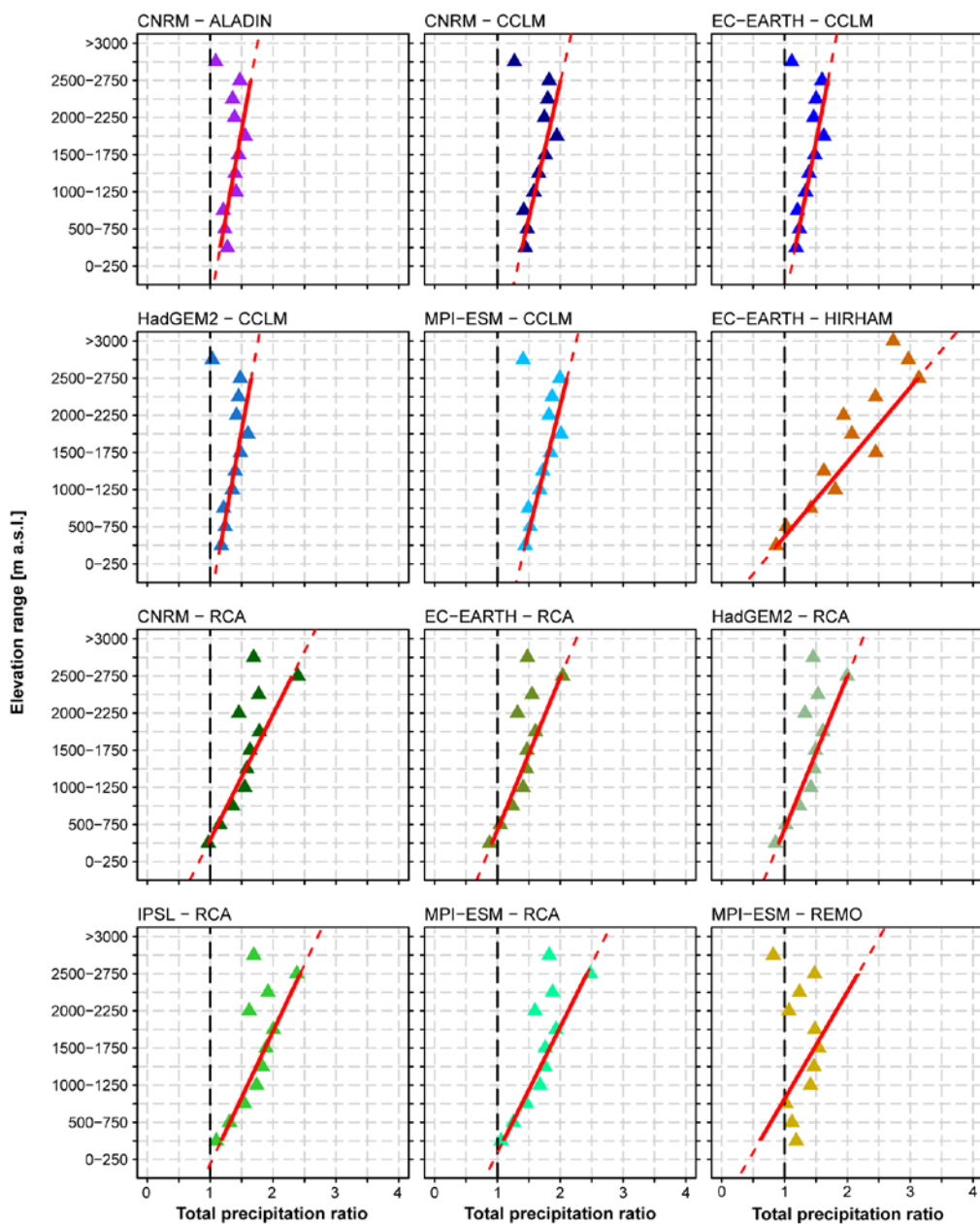


1327

1328  
1329  
1330  
1331

**Figure S2** Elevation-area distribution of the Alpine analysis domain (see Fig. 1 of the main manuscript) based on the high-resolution GTOPO30 digital elevation model (<https://ita.cr.usgs.gov/GTOPO30>) aggregated to a regular grid of 1.25 arc seconds (about 2 km). The area ratio provides the percentage contribution of a given elevation interval to the total area assuming equal grid cell areas.

1332



Comment [Sven11]: Figure revised due to removal of two further model chains.

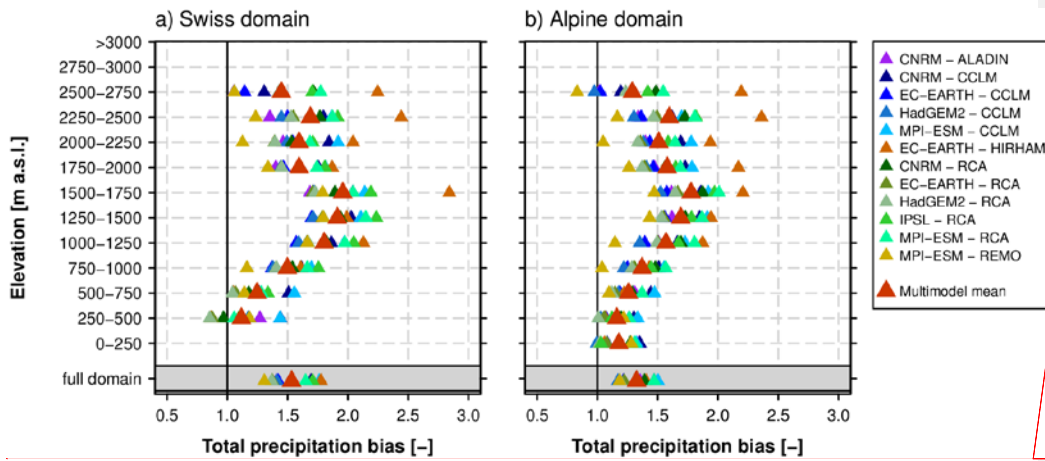
1333  
1334

1335 **Figure S3:** Ratios (RCM simulations divided by observational analysis) of total precipitation sums from  
1336 September to May in 1971 - 2005 vs. elevation for the Swiss domain. The linear regression line, applied to the  
1337 ratios for elevations between 250 m a.s.l. and 2750 m a.s.l., is represented by the red line.



1338

1339



Comment [Sven12]: Figure revised due to removal of two further model chains.

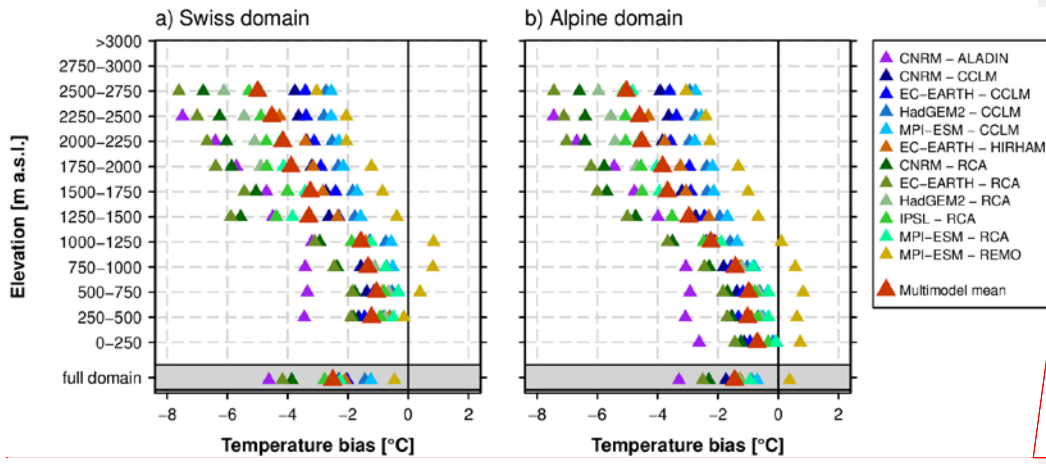
1340

1341 **Figure S4:** Total winter (SEP-MAY) precipitation bias (expressed as quotient between RCM simulations and  
1342 observations) in the EVAL period 1971-2005 for individual elevation intervals and for the full domain (lowermost  
1343 row). Left panel: Swiss domain only. Right panel: Entire Alpine analysis domain (cf. Fig. 1). Observational  
1344 reference: EOBS version 13.1 (Haylock et al., 2008) on 0.22° interpolated to the 0.11° RCM grid by nearest  
1345 neighbour interpolation.

1346

1347

1348

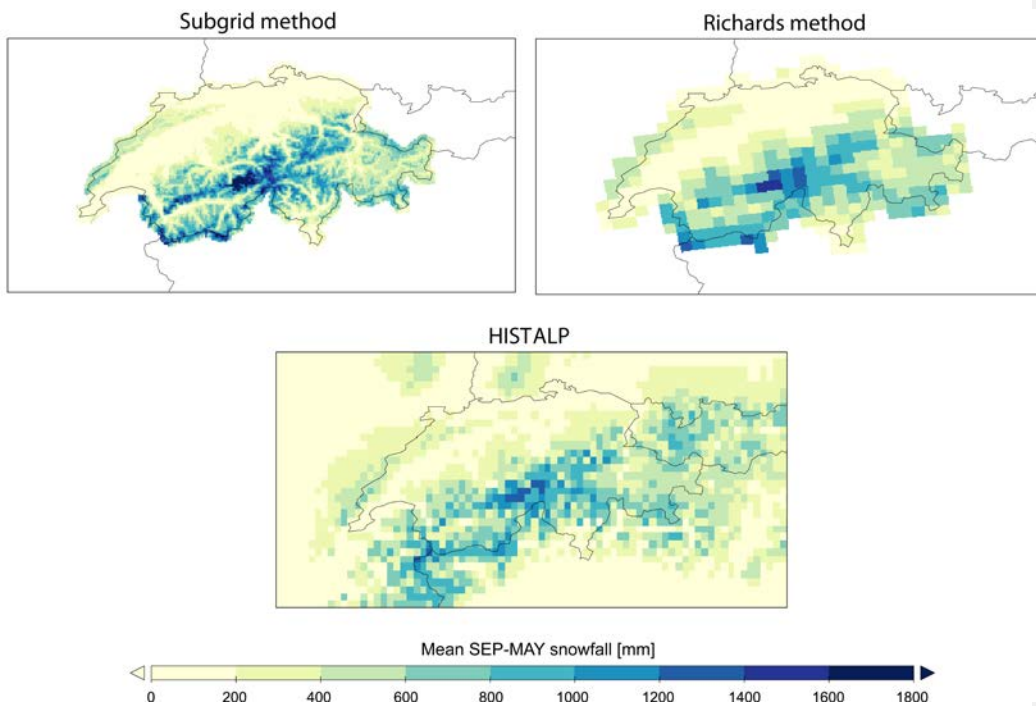


Comment [Sven13]: Figure revised due to removal of two further model chains.

1349

1350 **Figure S5:** As Figure S4 but for the winter (SEP-MAY) temperature bias.

1351



1352

1353

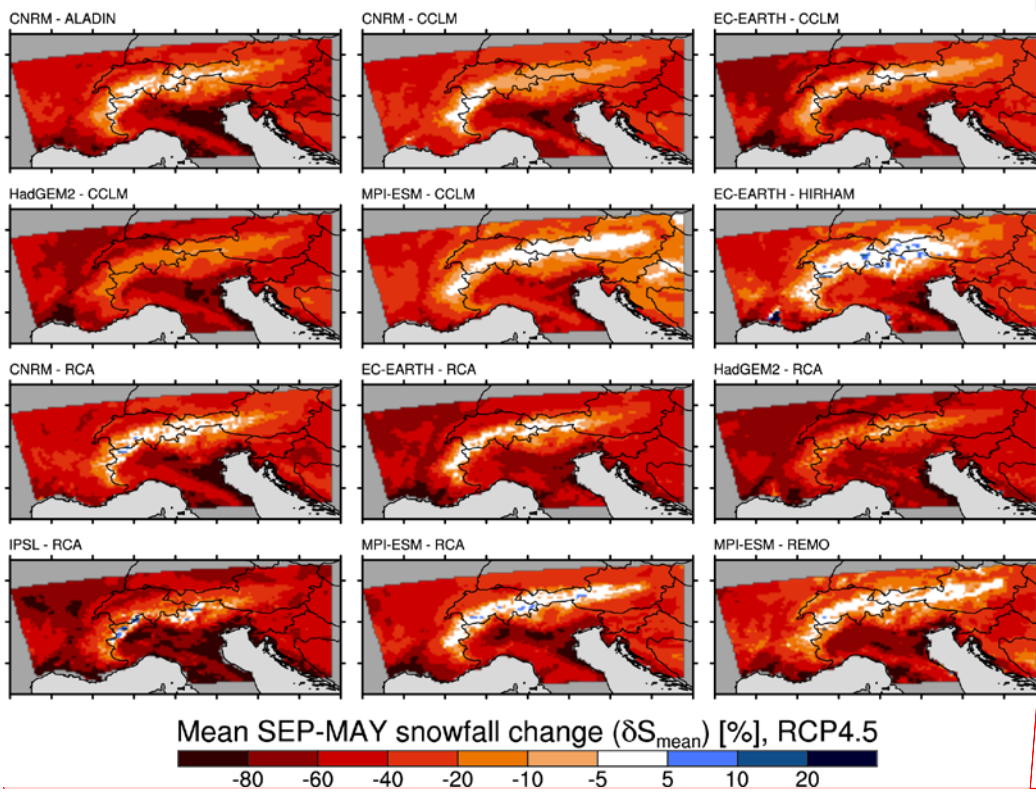
1354

1355

**Figure S6** Mean September-May snowfall sum [mm] in the period 1971-2005 as represented by the 2 km snowfall reference (*Subgrid method*; upper left), the 12 km snowfall reference on the RCM grid (*Richards method*; upper right) and the HISTALP dataset (Chimani et al., 2011; lower).

1356

1357



Comment [Sven14]: Figure revised due to removal of two further model chains.

1358

1359

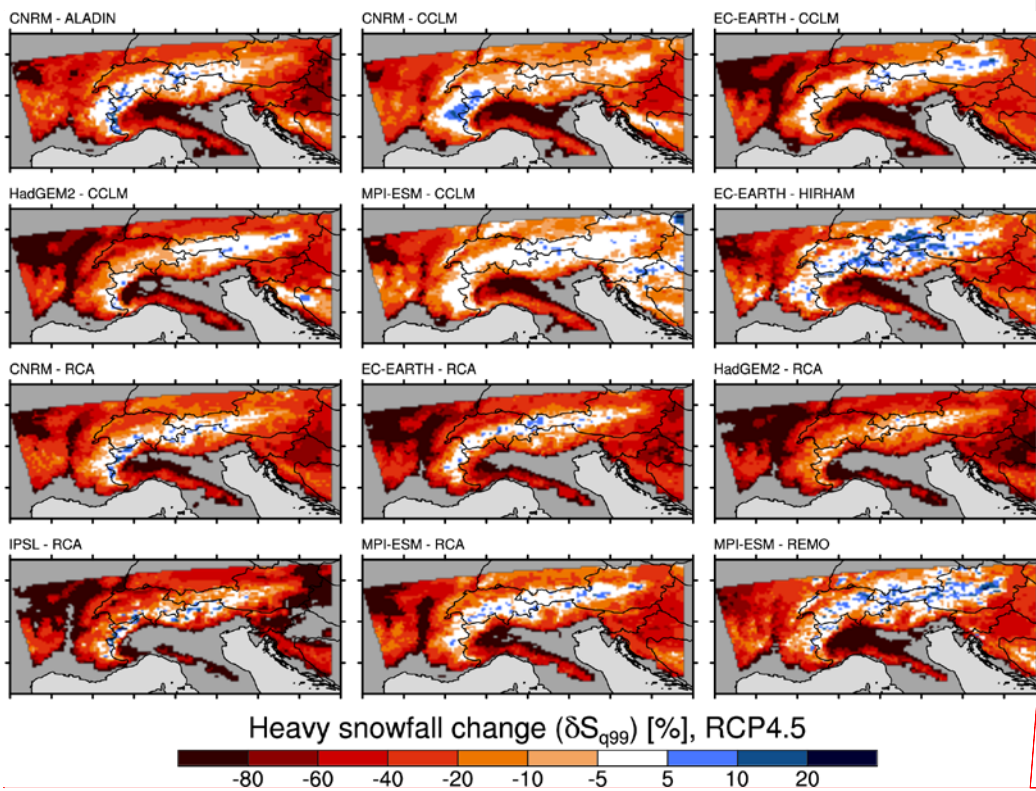
1360

1361

1362

1363

**Figure S7** Spatial distribution of relative changes (SCEN period 2070-2099 with respect to CTRL period 1981-2010) in mean September-May snowfall,  $\delta S_{\text{mean}}$ , for RCP4.5 and for the 12 snowfall separated + bias-adjusted RCM simulations ( $\text{RCM}_{\text{sep+ba}}$ ).



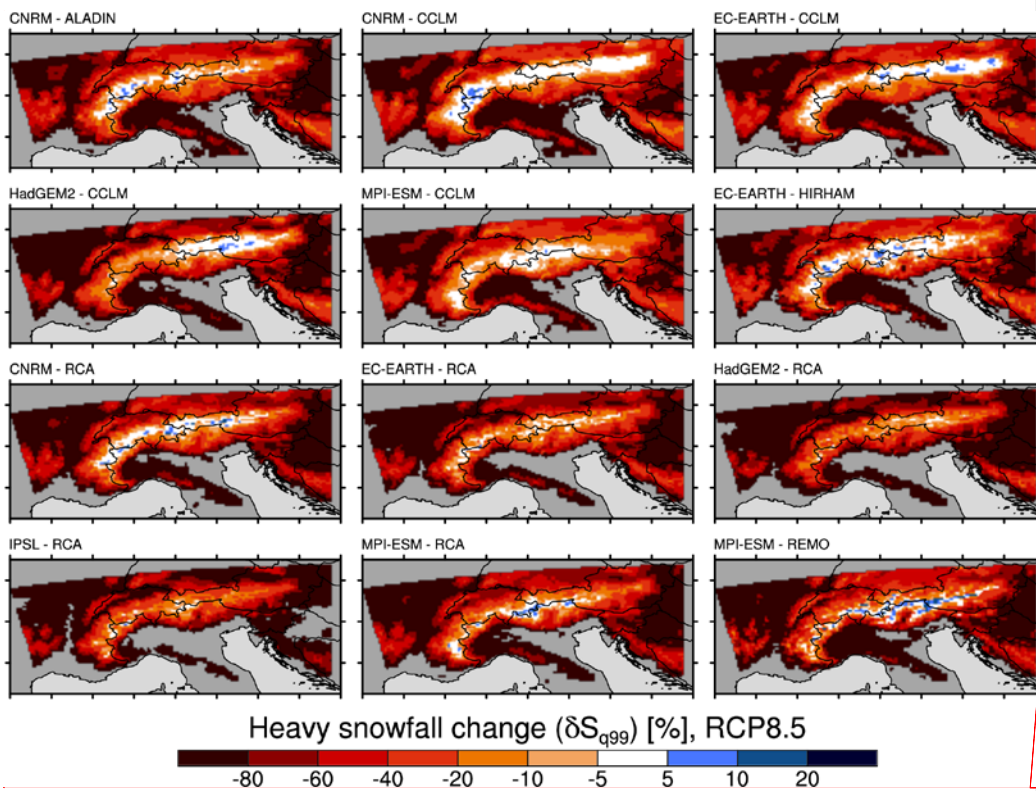
Comment [Sven15]: Figure revised due to removal of two further model chains.

1364  
1365

1366  
1367  
1368

**Figure S8** Spatial distribution of relative changes (SCEN period 2070-2099 with respect to CTRL period 1981-2010) in heavy snowfall,  $\delta S_{q99}$ , for RCP4.5 and for the 12 snowfall separated + bias-adjusted RCM simulations ( $RCM_{sep+ba}$ ).

1369



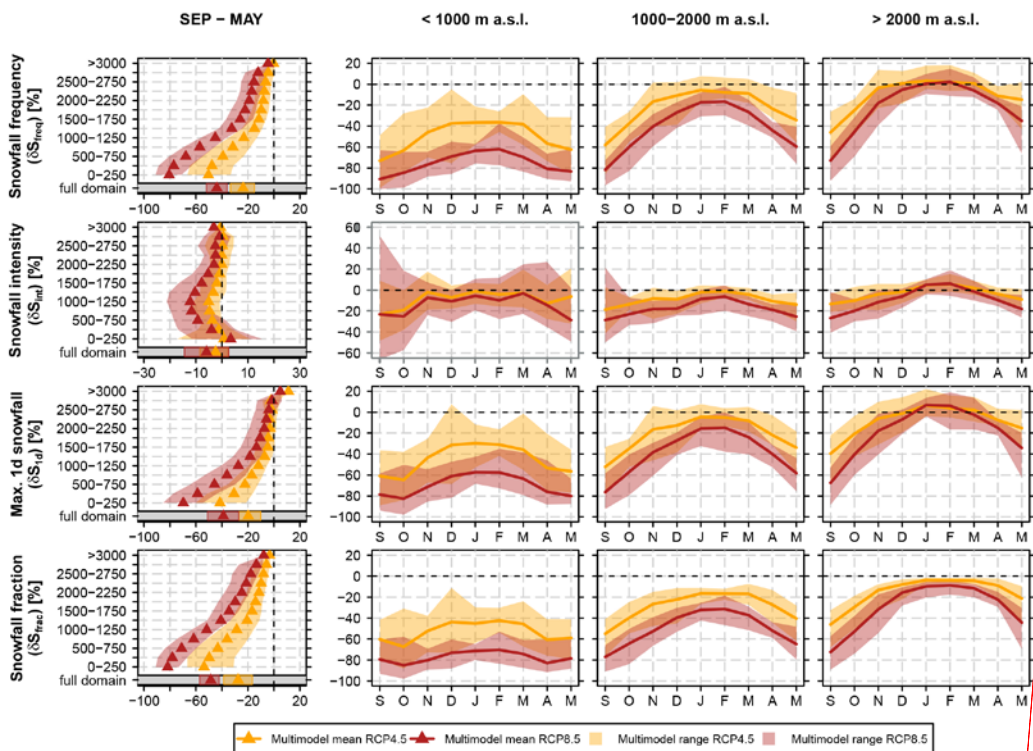
Comment [Sven16]: Figure revised due to removal of two further model chains.

1370  
1371

1372 **Figure S9** Spatial distribution of relative changes (SCEN period 2070-2099 with respect to CTRL period 1981-  
1373 2010) in heavy snowfall,  $\delta S_{q99}$ , for RCP8.5 and for the 12 snowfall separated + bias-adjusted RCM simulations  
1374 ( $RCM_{sep+ba}$ ).

1375





Comment [Sven17]: Figure revised due to removal of two further model chains.

1376  
1377

1378  
1379  
1380  
1381  
1382  
1383

**Figure S10** Relative changes (SCEN period 2070-2099 with respect to CTRL period 1981-2010) of max. 1 day snowfall,  $\delta S_{1d}$ , snowfall frequency,  $\delta S_{freq}$ , snowfall intensity,  $\delta S_{int}$ , and snowfall fraction,  $\delta S_{frac}$ , based on the 12 snowfall separated + bias-adjusted ( $RCM_{sep+ba}$ ) RCM simulations for RCP4.5 and RCP8.5, each. The first column shows the mean September-May snowfall index statistics vs. elevation while monthly snowfall index changes (spatially averaged over the elevation intervals  $<1000$  m a.s.l.,  $1000$  m a.s.l.- $2000$  m a.s.l. and  $>2000$  m a.s.l.) are displayed in columns 2-4.

1384  
1385